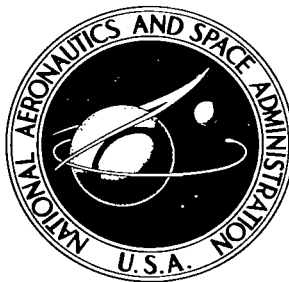


NASA TECHNICAL NOTE



NASA TN D-2575

c.1



NASA TN D-2575

SOME ASPECTS OF THE DISTRIBUTION OF METEORIC FLUX ABOUT AN ATTRACTIVE CENTER

by R. D. Shelton, H. E. Stern, and D. P. Hale
George C. Marshall Space Flight Center
Huntsville, Ala.



0079738

SOME ASPECTS OF THE DISTRIBUTION OF METEORIC
FLUX ABOUT AN ATTRACTIVE CENTER

By R. D. Shelton, H. E. Stern, and D. P. Hale

George C. Marshall Space Flight Center
Huntsville, Ala.

NATIONAL AERONAUTICS AND SPACE ADMINISTRATION

For sale by the Office of Technical Services, Department of Commerce,
Washington, D.C. 20230 -- Price \$3.00



TABLE OF CONTENTS

	Page
SUMMARY	1
SECTION I. INTRODUCTION	1
SECTION II. APPLICATION OF LIOUVILLE'S THEOREM TO MONO- ENERGETIC ISOTROPIC DISTRIBUTIONS	4
SECTION III. TREATMENT OF MONODIRECTIONAL, MONOENERGETIC DISTRIBUTIONS	13
A. Structure of the Flux Field for the Monoenergetic, Monodirectional Case	21
1. Basic Trajectory Geometry and Perspective	21
2. The Flux Zones	25
3. The Conjugate Trajectories	31
4. Exhibition of the Flux Field	34
B. Verification by Direct Calculation of the Result Obtained from the Application of Liouville's Theorem to Monoenergetic Isotropic Distributions	37
C. Effect of Detector Motion on Impact Rate	40
SECTION IV. CONCLUSION	50

LIST OF ILLUSTRATIONS

Figure	Title	Page
1	The Effect of the Earth on the Particle Kinetic Energy	5
2	The Shielding Effect of the Earth	9
3	The Shielding Effect of the Earth on the Flux for a Monoenergetic Isotropic Distribution	11
4	Flux Distribution for the Assumption of Isotropy at $r_O = 2r_E$	14
5	Flux Distribution for the Assumption of Isotropy at $r_O = 4r_E$	15
6	Behavior of a Monoenergetic, Monodirectional Distribution in the Vicinity of the Earth	16
7	Relative Number of Particles Intercepted by the Earth as a Function of Meteoroid Velocity at Infinity	18
8	The Relationship of the Element of Track Length ds to the Conservation of Angular Momentum	19
9	Perigee and Basic Angles	22
10	Geometrical Identification	26
11	Flux Zones of Upper Hemisphere	28
12	Relations Between the α 's	30
13	Conjugate Trajectories	33
14	Transformation of Spatial Coordinates	41
15	Transformation of Velocity Coordinates	43
16	The Effect of Detector Motion on Direction of Arrival of Meteoroids . .	44
17	The Effect of Detector Motion on Impact Speed of Meteoroids	45
18	The Effect of Detector Motion on a Monoenergetic, Monodirectional Flux	49

LIST OF ILLUSTRATIONS (Cont'd)

Figure	Title	Page
19	The Influence of Detector Motion on Apparent Flux. The Distribution in the Fixed System is Assumed to be Monoenergetic, Spatially Uniform, and Isotropic	51
20	The Effect of Detector Motion on the Kinetic Energy for Monoenergetic, Monodirectional Flux	52
21	The Effect of Detector Motion on the Average Kinetic Energy for an Isotropic Monoenergetic Distribution	53

TECHNICAL NOTE D-
SOME ASPECTS OF THE DISTRIBUTION OF METEORIC
FLUX ABOUT AN ATTRACTIVE CENTER¹

SUMMARY

The discussion is in the form of a general survey to illustrate the magnitude and nature of some of the problems associated with measuring meteoroid flux from moving satellites. The application of the Liouville theorem represents an extension of a practice common to the treatment of charged particles in electromagnetic fields and the treatment of the structure of the flux field constitutes an extension of the asymptotic discussion of the Rutherford scattering problem involving Coulomb repulsion to the region near an attracting force center. The problem of the orientation of a non-spherical detector is not considered.

An attempt will be made to apply the techniques developed here to the detailed interpretation of the count rate measured by the Saturn boosted micrometeoroid satellite. Statistical methods must of course be developed to bridge the gap between the analytic streams assumed here and the paucity of counts expected from the coming experiment.

A mathematical basis for discussing such subjects as the focusing of meteoroids by the earth has been provided, but considerable work still remains on the problem of using measured distributions, with no velocity or direction information, to estimate the meteoroid flux at infinity.

SECTION I. INTRODUCTION

The impact of meteoroids on a spacecraft will depend on the meteoroid distribution and the location and the state of motion of the spacecraft. One can argue on an intuitive basis that the gravitational field of the earth will concentrate the meteoroids in the vicinity of the earth and that meteoroids near the earth will be moving faster because of the gain in kinetic energy available from the earth's gravitational field. It is evident also that motion of the spacecraft will change the apparent direction and rate of the meteoroid

¹. Paper presented at the COSPAR Fourth International Space Science Symposium, Warsaw, Poland, June 3-12, 1963.

impact, as well as altering the energy and momentum exchange on impact. If the meteoroid distribution is not isotropic in direction and the spacecraft is not a sphere, it is quite possible that the orientation of the spacecraft can be important in determining the meteoroid impact rate.

In discussing the several phenomena of interest, it is convenient to employ a distribution function $N(\bar{r}, \bar{v})$ in position and velocity space such that the expression,

$$N(\bar{r}, \bar{v}) \overline{dr dv}, \quad (1)$$

represents the number of particles contained in the six-dimensional element of volume $\overline{dr dv}$, where \bar{r} is the position vector, drawn from the earth, and \bar{v} is the velocity vector. Because the mass of a particle does not affect its motion in the gravitational field of the earth, the distribution over mass is not considered. The particle density $N(\bar{r})$ is given by the integral of $N(\bar{r}, \bar{v})$ over velocity space, that is,

$$N(r) = \int \int N(\bar{r}, \bar{v}) \overline{dv} . \quad (2)$$

The particle flux, numerically equal to the impact rate on a sphere which presents unit area to all directions, is defined as

$$\phi(r) = \int \int v N(\bar{r}, \bar{v}) \overline{dv} \quad (3)$$

where v is the magnitude of the velocity vector \bar{v} . The directional flux, or vector current density $J(r, \hat{v})$ is given by

$$J(r, \hat{v}) = \int \bar{v} N(\bar{r}, \bar{v}) \overline{dv} \quad (4)$$

where \hat{v} is a unit vector along \bar{v} .

Flux is a generalization of the current concept and reduces to the magnitude of the current vector when the corpuscles are incident upon an infinitesimal surface or volume from a single direction. When particles are incident simultaneously from two or more directions - as they are in meteoric, cosmic ray, nuclear radiation, and all isotropic fields - one can perform a useful summation¹ over all of the currents by defining

1. Summation is not vectorial but is over the magnitudes of the current vectors.

the flux as the

total particle path - length traced out per unit volume, at the point of interest, during unit time.

Since a cylinder whose base is of unit area, and whose height is $|\bar{v}_i|$, containing ρ_i particles per unit volume, can be regarded as flowing through the unit volume during unit time, where

\bar{v}_i = the velocity of the particles incident from ith direction

ρ_i = the density of the particles incident from ith direction,

the path length generated within the unit volume during unit time is clearly $\rho_i v_i$. We can write the flux ϕ as

$$\phi \equiv \sum_i \rho_i v_i = \sum_i |J_i| \quad (\bar{J}_i \text{ the current due to particles from } i \text{ direction})$$

In the case of particles incident from a single direction, this reduces to the current J or number of particles crossing unit area normal to the current, during unit time, i. e., $\phi \rightarrow |J|$.

The number of particles crossing a unit area per unit time is given by

$$J(\bar{r}, \hat{\Omega}) = \int \int \hat{\Omega} \bar{J}(\bar{r}, \hat{v}) d\omega \quad (5)$$

where $\hat{\Omega}$ is the outward normal unit vector to the area and $d\omega$ is the element of the solid angle. The integral over ω is to be carried out over a 2π solid angle to obtain the impact rate on one side of the area.

The problem posed is that of determining how $N(r, v)$ and the associated quantities $N(\bar{r})$, $\phi(\bar{r})$, $\bar{J}(\bar{r}, \hat{v})$ and $J(\bar{r}, \hat{\Omega})$ are changed by the presence of the earth and the motion of a satellite designed to measure them. The law of energy conservation permits us to write

$$v_\infty^2 + 2\gamma M/r = v^2(r) \quad (6)$$

where v_∞ is the particle speed at infinity, γ is the gravitational constant, M is the mass of the earth, and $v(r)$ is the particle speed at a distance r from the earth. The law of conservation of angular momentum permits us to write

$$|\bar{\mathbf{r}} \times \bar{\mathbf{v}}| = a v_{\infty} \quad (7)$$

where a is the impact parameter and \mathbf{r} and \mathbf{v} are the position and velocity vectors at any point on a particle orbit.

From Equation 6, we see that the impact problem is more severe near the earth than in free space, because of the additional speed associated with the entry of the particle into the gravitational field of the earth. Further, we can see that a monoenergetic distribution at infinity is monoenergetic everywhere, with the correct speed given by Equation 6. In Figure 1, the dependence of kinetic energy on distance from the earth is shown graphically. The escape velocity v_e is given by

$$v_e = \sqrt{2 \gamma M / r_E} = 1.1 \times 10^4 \text{ m/sec}, \quad (8)$$

where r_E is the radius of the earth, has been chosen as a convenient reference velocity. Figure 1 illustrates well the expectation that high velocity meteoroids are influenced relatively little by the earth.

SECTION II. APPLICATION OF LIOUVILLE'S THEOREM TO MONOENERGETIC ISOTROPIC DISTRIBUTIONS

The Liouville theorem states that the density of particles in the neighborhood of a given particle in phase space does not change as a result of the particle motion. Therefore, if $(\bar{\mathbf{r}}_1, \bar{\mathbf{v}}_1)$ and $(\bar{\mathbf{r}}_2, \bar{\mathbf{v}}_2)$ are two points in phase space which lie on a particle trajectory, then

$$N(\bar{\mathbf{r}}_1, \bar{\mathbf{v}}_1) = N(\bar{\mathbf{r}}_2, \bar{\mathbf{v}}_2) \quad . \quad (9)$$

The distribution function $N(\bar{\mathbf{r}}, \bar{\mathbf{v}})$ may be taken as the phase space density, although it is more common to use the momentum rather than the velocity coordinates. The Liouville theorem can be applied to show that, if the distribution of particles is uniform, isotropic in direction, and monoenergetic at infinity, it is monoenergetic and isotropic everywhere. This can be seen by examining the possible trajectories which can be drawn through a point located by the position vector $\bar{\mathbf{r}}$, which locates the point relative to the earth. Through this point, trajectories can be drawn in all possible directions and traced to infinity, subject only to the constraint that everywhere

$$v(\bar{\mathbf{r}}) \geq v_e \equiv \sqrt{2 \gamma M / r} \quad , \quad (10)$$

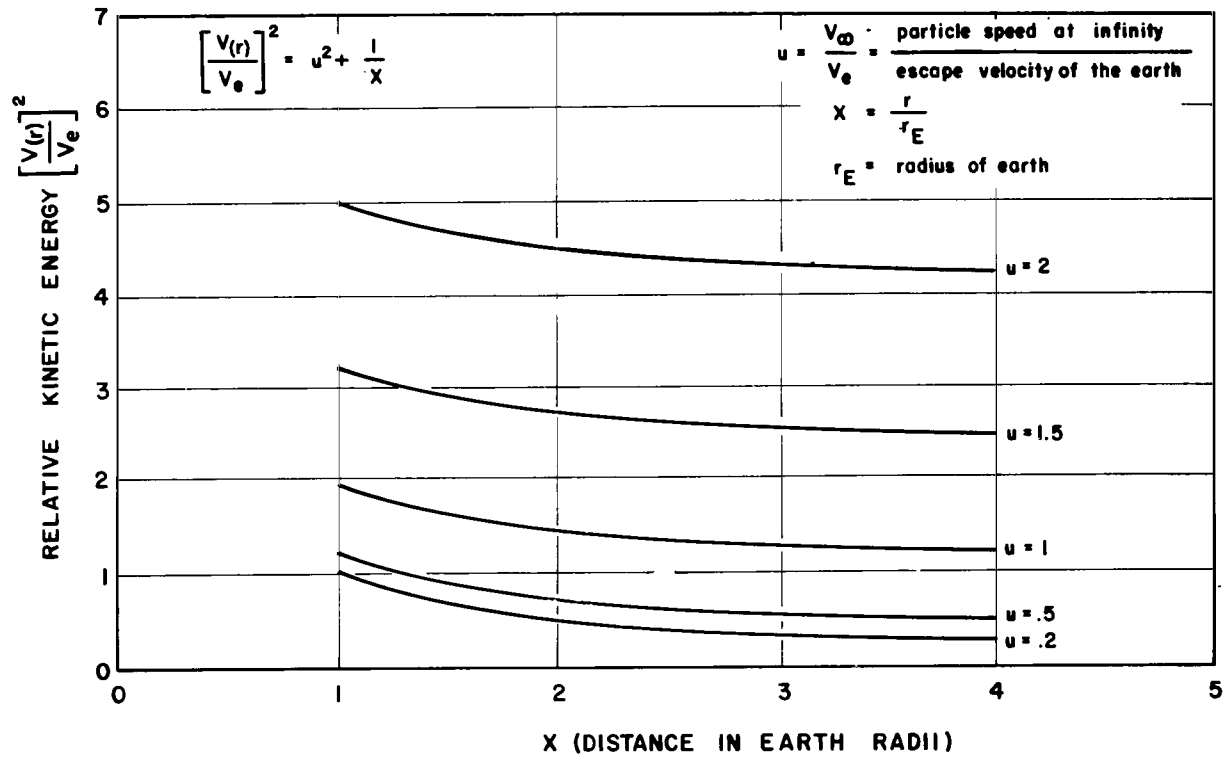


FIGURE 1. THE EFFECT OF THE EARTH ON THE PARTICLE KINETIC ENERGY

v_e being the velocity of escape at any point \bar{r} . If the two points in Equation 9 are considered to be located at \bar{r} and at infinity, every possible direction at \bar{r} can be connected to infinity, where the distribution is isotropic, monoenergetic, and uniform, and where the particle density in phase space, by the Liouville theorem is the same as at \bar{r} .

Let us assume that the distribution function at \bar{r}_1 in Equation 9 can be written in the form of a Dirac delta function,

$$N(\bar{r}_1, \bar{v}_1) = c \delta [v_1 - v(r_1)] \quad . \quad (11)$$

where c is a constant, v_1 is the variable of distribution, and $v(r_1)$ is a speed parameter. Equation 11 states that the distribution at \bar{r}_1 is isotropic, spherically symmetric, and monoenergetic, with all particles having a speed $v(r_1)$. In terms of spherical coordinates, the element of volume in velocity space can be written as

$$dv_1 = v_1^2 dv_1 \sin \theta_1 d\theta_1 d\phi_1 \quad . \quad (12)$$

From Equation 2 the particle density is given by

$$\begin{aligned} N(r_1) &= \int_{v_1=0}^{v_1=\infty} \int_{\theta_1=0}^{\theta_1=\pi} \int_{\phi_1=0}^{\phi_1=2\pi} c \delta [v_1 - v(r_1)] v_1^2 dv_1 \sin \theta_1 d\theta_1 d\phi_1 \\ &= 4\pi c v^2(r_1) \quad . \end{aligned} \quad (13)$$

At \bar{r}_2 , another point on a trajectory through \bar{r}_1 , Equations 2, 9, 11, and 12 permits us to write an expression for the particle density in the form

$$\begin{aligned} N(\bar{r}_2) &= \int_{v_2=0}^{v_2=\infty} \int_{\theta_2=0}^{\theta_2=\pi} \int_{\phi_2=0}^{\phi_2=2\pi} N(\bar{r}_2, \bar{v}_2) v_2^2 \sin \theta_2 dv_2 d\theta_2 d\phi_2 \\ &= \int_{v_2=0}^{v_2=\infty} \int_{\theta_2=0}^{\theta_2=\pi} \int_{\phi_2=0}^{\phi_2=2\pi} N(\bar{r}_1, \bar{v}_1) v_2^2 \sin \theta_2 dv_2 d\theta_2 d\phi_2 \\ &= \int_{v_2=0}^{v_2=\infty} \int_{\theta_2=0}^{\theta_2=\pi} \int_{\phi_2=0}^{\phi_2=2\pi} c \delta [v_1 - v(r_1)] v_2^2 \sin \theta_2 dv_2 d\theta_2 d\phi_2 \end{aligned}$$

$$= 4\pi \text{ c } \int_{v_2=0}^{v_2=\infty} \delta [v_1 - v(r_1)] v_2^2 dv_2 . \quad (14)$$

If, in particular, we assume that the distribution represented by Equation 11 results from an isotropic, uniform, monoenergetic distribution at infinity and that the particle speeds v_1 and v_2 are related through Equation 6 for the conservation of energy, we have

$$v_1^2 - 2\gamma M/r_1 = v_2^2 - 2\gamma M/r_2 \quad (15)$$

so that

$$v_1 dv_1 = v_2 dv_2 \quad (16)$$

The substitution of Equations 15 and 16 into Equation 14 yields¹

$$\begin{aligned} N(\bar{r}_2) &\doteq 4\pi \text{ c } \int_{v_1=\sqrt{2\gamma M [(r_2 - r_1)/(r_1 r_2)]}}^{v_1=\infty} \delta [v_1 - v(r_1)] v_2 v_1 dv_1 \\ &= 4 \pi \text{ c } v(r_2) v(r_1) \end{aligned} \quad (17)$$

The ratio of particle densities at \bar{r}_2 and \bar{r}_1 is given by Equations 13 and 17 as

$$N(\bar{r}_2)/N(\bar{r}_1) = v(\bar{r}_2)/v(\bar{r}_1) . \quad (18)$$

If r_1 is assumed to be at infinity and r_2 is arbitrary, the application of Equation 6 results in

$$N(\bar{r})/N(\infty) = v(\bar{r})/v(\infty) = [1 + 2\gamma M/rv_\infty^2]^{1/2} . \quad (19)$$

In a like manner, the ratio of fluxes is found to be

$$\phi(\bar{r})/\phi(\infty) = [1 + 2\gamma M/rv_\infty^2] . \quad (20)$$

¹. alternatively this can be regarded as transformation - i. e. , Jacobian $J(v_2/v_1) = v_1/v_2$ to obtain the same result.

In the vicinity of a finite earth, the meteoroid density and flux predicted by Equations 19 and 20 are reduced by the shielding effect of the earth. In Figure 2, the point P at which the flux is to be computed is located at a distance r from the earth. Particles which would have arrived at an angle of less than θ_m have been intercepted by the earth. The correction factor F for Equations 19 and 20, for the case of isotropic radiation, is just the ratio of the solid angle over which radiations can arrive to the total solid angle above the point. Therefore

$$F = \frac{\int_{\theta=\theta_m}^{\theta=\pi} \sin \theta d\theta}{\int_{\theta=0}^{\theta=\pi} \sin \theta d\theta} = 1/2 [1 + \cos \theta_m] \quad (21)$$

Using Equation 7, the definition of the vector cross product, and the fact that \bar{r} and \bar{v} are normal at the point of closest approach r_E , as shown in Figure 2, θ_m may be defined by the equation,

$$a_m v_\infty = r_E v_E = r v(r) \sin \theta_m, \quad (22)$$

where a_m is the impact parameter associated with the grazing orbit, and the conservation of momentum is applied to three points located on the grazing orbit. From Equations 6 and 22,

$$\begin{aligned} \sin \theta_m &= [r_E v_E] / [r v(r)] \\ &= \frac{r_E}{r} \left[\frac{v_\infty^2 + 2\gamma M/r_E}{v_\infty^2 + 2\gamma M/r} \right]^{1/2} \end{aligned} \quad (23)$$

and

$$\begin{aligned} F &= (1 + \cos \theta_m)/2 = (1 + [1 - \sin^2 \theta_m]^{1/2})/2 \\ &= \frac{1}{2} \left\{ 1 + \left[1 - \left(\frac{r_E}{r} \right)^2 \left(\frac{v_\infty^2 + 2\gamma M/r_E}{v_\infty^2 + 2\gamma M/r} \right) \right]^{1/2} \right\} \end{aligned} \quad (24)$$

With this correction factor, Equation 20 now becomes¹

¹. Compare with S. F. Singer, Nature, Vol. 192, No. 4800, pp. 321-323, October 1961, where several of the techniques used here are employed in a less extensive development.

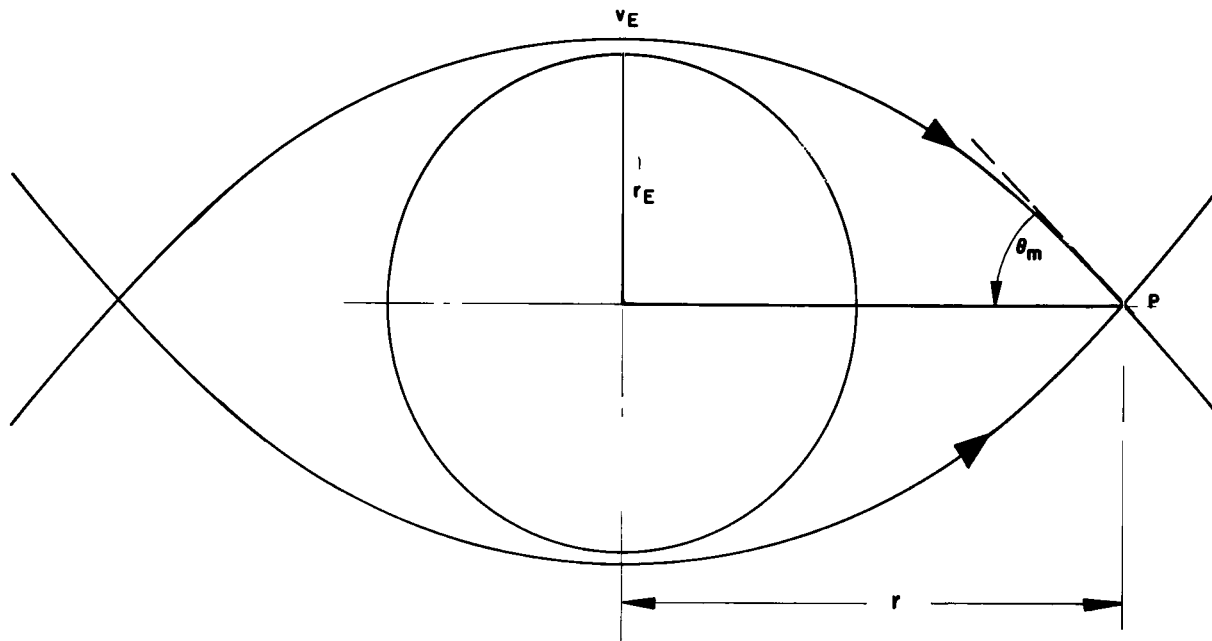


FIGURE 2. THE SHIELDING EFFECT OF THE EARTH

$$\phi(r)/\phi(\infty) = [1 + 2\gamma M/r v_\infty^2] \left\{ 1 + \left[1 - \left(\frac{r_E}{r} \right)^2 \left(\frac{v_\infty^2 + 2\gamma M/r_E}{v_\infty^2 + 2\gamma M/r} \right) \right]^{1/2} \right\} / 2 \quad (25)$$

By making the substitutions,

$$x = r/r_E \quad , \quad (26)$$

$$v_e^2 = 2\gamma M/r_E \quad , \quad (27)$$

$$u = v_\infty/v_e \quad , \quad (28)$$

we can write Equation 25 as

$$\phi(r)/\phi(\infty) = \frac{1}{2} \left[\frac{1 + xu^2}{xu^2} \right] \left\{ 1 + \left[1 - \frac{(u^2 + 1)}{x(u^2 x + 1)} \right]^{1/2} \right\}. \quad (29)$$

In Figure 3, $\phi(r)/\phi(\infty)$ is graphed as a function of x with u as a parameter.

In dealing with particles in orbit about the earth, let us make the assumption that the distributions are isotropic in direction except for directions which are excluded because the corresponding particle orbits intersect the earth. For the particle to be captured, we must have $v(r) \leq 2\gamma M/r$ everywhere, which corresponds to a negative total energy. The results are much the same as before, except that we can no longer choose the reference point at infinity and we must exclude both incoming and outgoing particles whose orbits intersect the earth.

If r_0 is chosen as the reference point, Equation 20 is written as

$$\phi(\bar{r})/\phi(r_0) = F v^2(r)/v_0^2 \quad (30)$$

where F is a correction factor and v_0 is the speed at r_0 . Because incoming and outgoing orbits should be eliminated from the flux contributions, at both the reference point and the observation point, Equation 21 becomes

$$F = \frac{\int_{\theta=\theta_m}^{\theta=\pi-\theta_m} \sin \theta d\theta}{\int_{\theta=\theta_0}^{\theta=\pi-\theta_0} \sin \theta d\theta} = \frac{\cos \theta_m}{\cos \theta_0} \quad . \quad (31)$$

From Equation 22

$$r_E v_E = r_0 v_0 \sin \theta_0 = r v \sin \theta_m \quad (32)$$

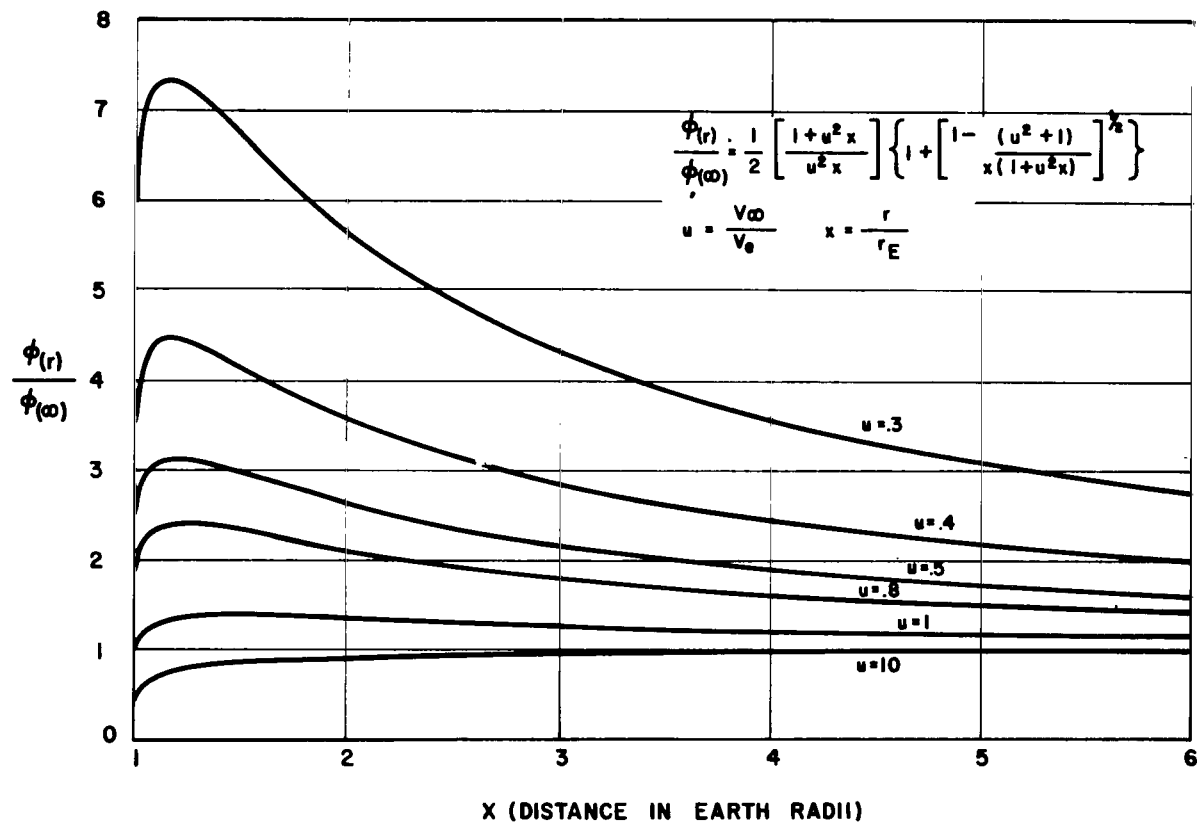


FIGURE 3. THE SHIELDING EFFECT OF THE EARTH ON THE FLUX FOR A MONOENERGETIC ISOTROPIC DISTRIBUTION

where θ_o and θ_m define the cones of intercepted trajectories at r_o and r respectively as shown in Figure 2, with

$$\theta_o < \theta < \pi - \theta_o, \sin \theta_o = r_E v_E / r_o v_o, \quad (33)$$

and the permissible directions at r given by

$$\theta_m < \theta < \pi - \theta_m, \sin \theta_m = r_E v_E / r v. \quad (34)$$

Therefore

$$F = \frac{\cos \theta_m}{\cos \theta_o} = \left[1 - \left(\frac{r_E v_E}{r v} \right)^2 \right]^{1/2} \left[1 - \left(\frac{r_E v_E}{r_o v_o} \right)^2 \right]^{-1/2} \quad (35)$$

and

$$\phi(r)/\phi(r_o) = \left(\frac{v}{v_o} \right)^2 \left[1 - \left(\frac{r_E v_E}{r v} \right)^2 \right]^{1/2} / \left[1 - \left(\frac{r_E v_E}{r_o v_o} \right)^2 \right]^{1/2} \quad (36)$$

From Equation 6

$$v_o^2 - 2\gamma M/r_o = v^2 - 2\gamma M/r \quad (37)$$

so that

$$v^2 = v_o^2 - 2\gamma M(1/r_o - 1/r) \quad (38)$$

and

$$v_E^2 = v_o^2 - 2\gamma M(1/r_o - 1/r_E) \quad (39)$$

Using Equations 26 and 27 and defining u and x_o by the equations

$$\begin{aligned} u &\equiv v_o/v_e, \\ x_o &\equiv r_o/r_E, \end{aligned} \quad (40)$$

we may use Equations 38 and 39 to write Equation 36 as

$$\phi(r)/\phi(r_0) = \left[\frac{1 + xu^2 - x/x_0}{xu^2} \right] \left[\frac{1 - \frac{(u^2 + 1 - 1/x_0)}{x(u^2x + 1 - x/x_0)}}{1 - \frac{u^2 + 1 - 1/x_0}{x_0^2 u^2}} \right]^{1/2} \quad (42)$$

Figures 4 and 5 show plots of $\phi(r)/\phi(r_0)$ as a function of radial distance from the earth for r_0 equal to two and four earth radii.

SECTION III. TREATMENT OF MONODIRECTIONAL, MONOENERGETIC DISTRIBUTIONS

A function describing the distribution of meteoroids in position and velocity space may be approximated by the superposition of a group of monodirectional monoenergetic distributions which have been given proper weight. In treating neutron and gamma transport problems, for example, it is common practice to approximate continuous distributions in energy by a number of weighted energy groups. Computers are used to obtain a solution for each energy group, and the solutions are added to yield a total solution.

Following the same practice, let us assume that we have an infinite plane emitting meteoroids in the positive x direction as shown in Figure 6. As the meteoroids approach a center of force, they increase in speed and are deflected from their straight line paths. The speed of the meteoroid as a function of position relative to the gravitating body is given by Equation 6, which is a statement of the conservation of energy.

The radiation intercepting a spherical surface of radius r can be computed simply from angular momentum considerations by using Equation 7. Equating the angular momentum at infinity to the angular momentum at the point of closest approach for a particle which just grazes the sphere of radius r , we obtain

$$v_\infty a = v(r) r \quad (43)$$

From Equation 6

$$v(r) = (2\gamma M/r + v_\infty^2)^{1/2} \quad (44)$$

so that, combining Equations 43 and 44 we have

$$a = (2\gamma M/r + v_\infty^2)^{1/2} r/v_\infty \quad (45)$$

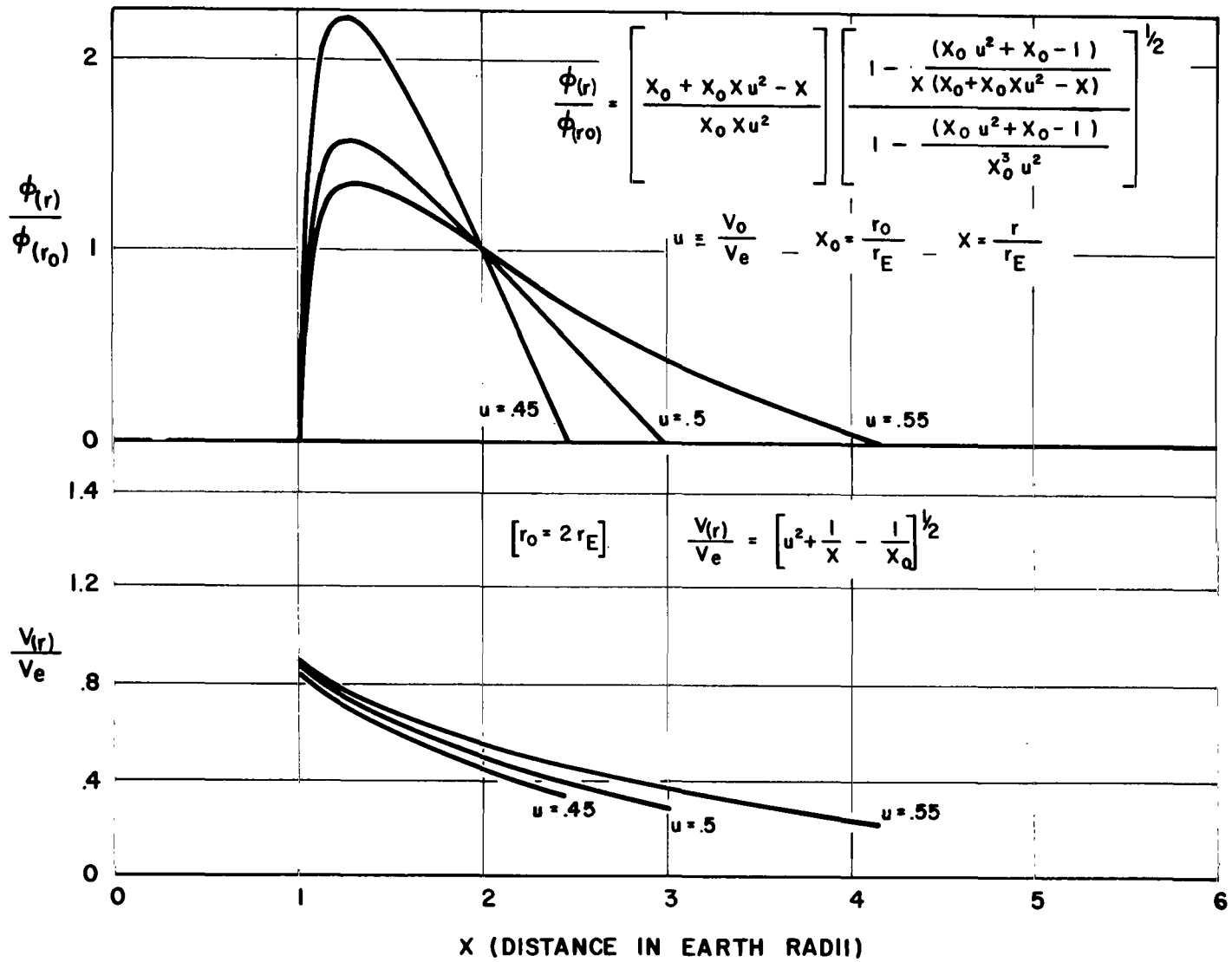


FIGURE 4. FLUX DISTRIBUTION FOR THE ASSUMPTION OF ISOTROPY AT $r_0 = 2r_E$

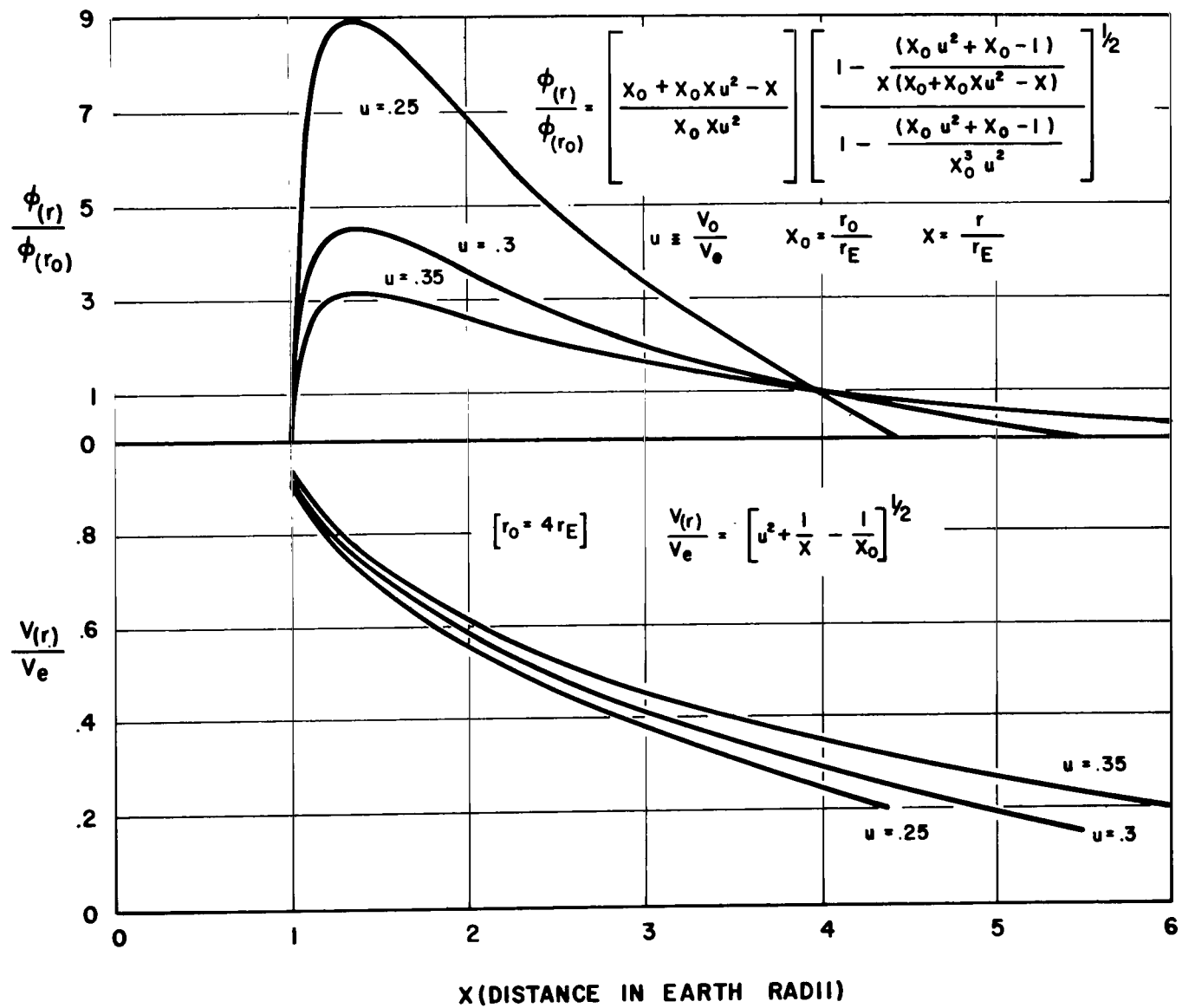


FIGURE 5. FLUX DISTRIBUTION FOR THE ASSUMPTION OF ISOTROPY AT $r_0 = 4r_E$

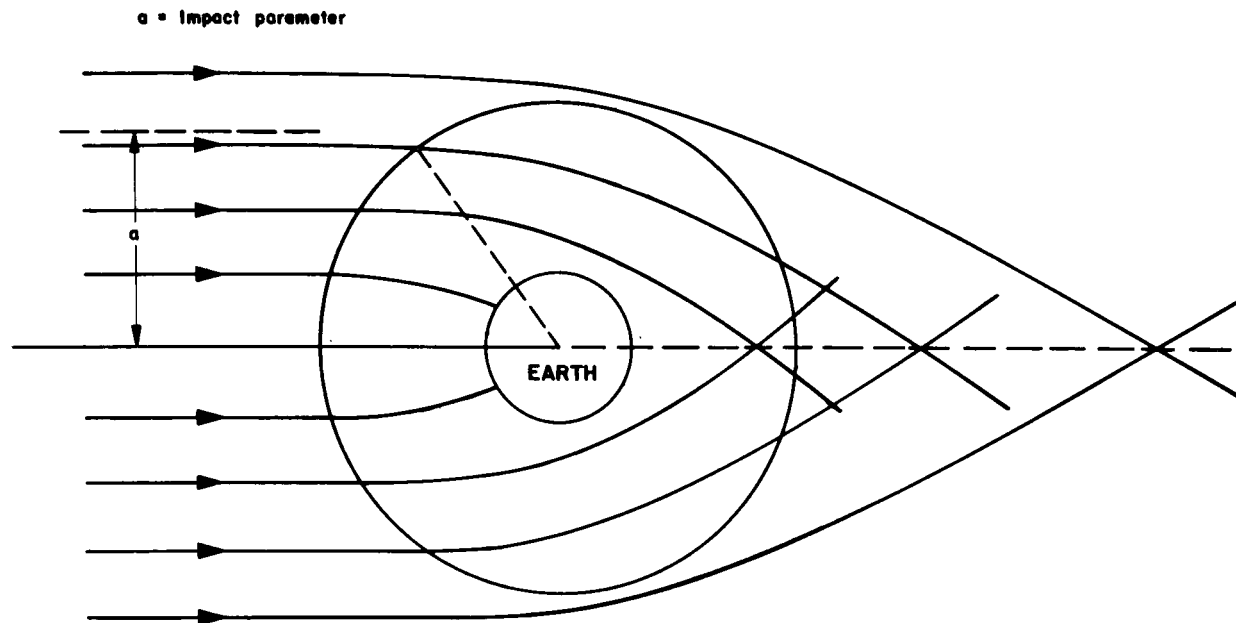


FIGURE 6. BEHAVIOR OF A MONOENERGETIC, MONODIRECTIONAL DISTRIBUTION IN THE VICINITY OF THE EARTH

All particles with smaller impact parameters will intersect the sphere of radius r . If the infinite plane emits meteoroids normally at the rate of c particles per unit area per unit time with speed v_∞ , the number intersecting the sphere of radius r is the number with impact parameters less than a , or

$$I = \pi a^2 c = \pi(1 + 2\gamma M/rv_\infty^2) cr^2 \quad (46)$$

The number intersecting the earth is given similarly by

$$I_E = \pi a_E^2 c = \pi(1 + 2\gamma M/r_E v_\infty^2) r_E^2 c = \pi r_E^2 c \left[1 + v_e^2/v_\infty^2 \right] \quad (47)$$

A plot of earth intercepts as a function of velocity at infinity is given in Figure 7. The same result (Equation 20) is obtained for the isotropic case, and this plot indicates the magnitude of some of the corrections needed for radar observations of incoming meteoroids.

The flux $\phi(\vec{r})$ at a point can be conveniently approached in terms of the path length per unit time per unit volume traced out by the particles as they move along trajectories. Imagine a differential volume $4\pi r^2 dr$ penetrated by a trajectory as in Figure 8. The path length created in this volume by a particle moving along the trajectory is given by

$$2 ds = 2 \sqrt{dr^2 + r^2 d\theta^2} = 2 \left[1 + r^2 (d\theta/dr)^2 \right]^{1/2} dr. \quad (48)$$

The factor of two is included because the orbital symmetry requires that the particle have the same track length on emerging from the shell. Although the track length can be evaluated formally from Equation 48 and the orbit equation, it is easier to use the conservation of momentum equation and write, from Equation 7,

$$|\vec{r} \times \vec{v}| = a v_\infty = r v \sin \alpha \quad (49)$$

where α is as shown in Figure 8. Therefore,

$$\sin \alpha = av_\infty/rv(r). \quad (50)$$

From Figure 8

$$dr = ds \cos \alpha \quad (51)$$

and

$$\begin{aligned} ds &= dr/\cos \alpha = dr/\left[1 - \sin^2 \alpha \right]^{1/2} \\ &= dr/\left[1 - \left(av_\infty/rv(r) \right)^2 \right]^{1/2} \end{aligned} \quad (52)$$

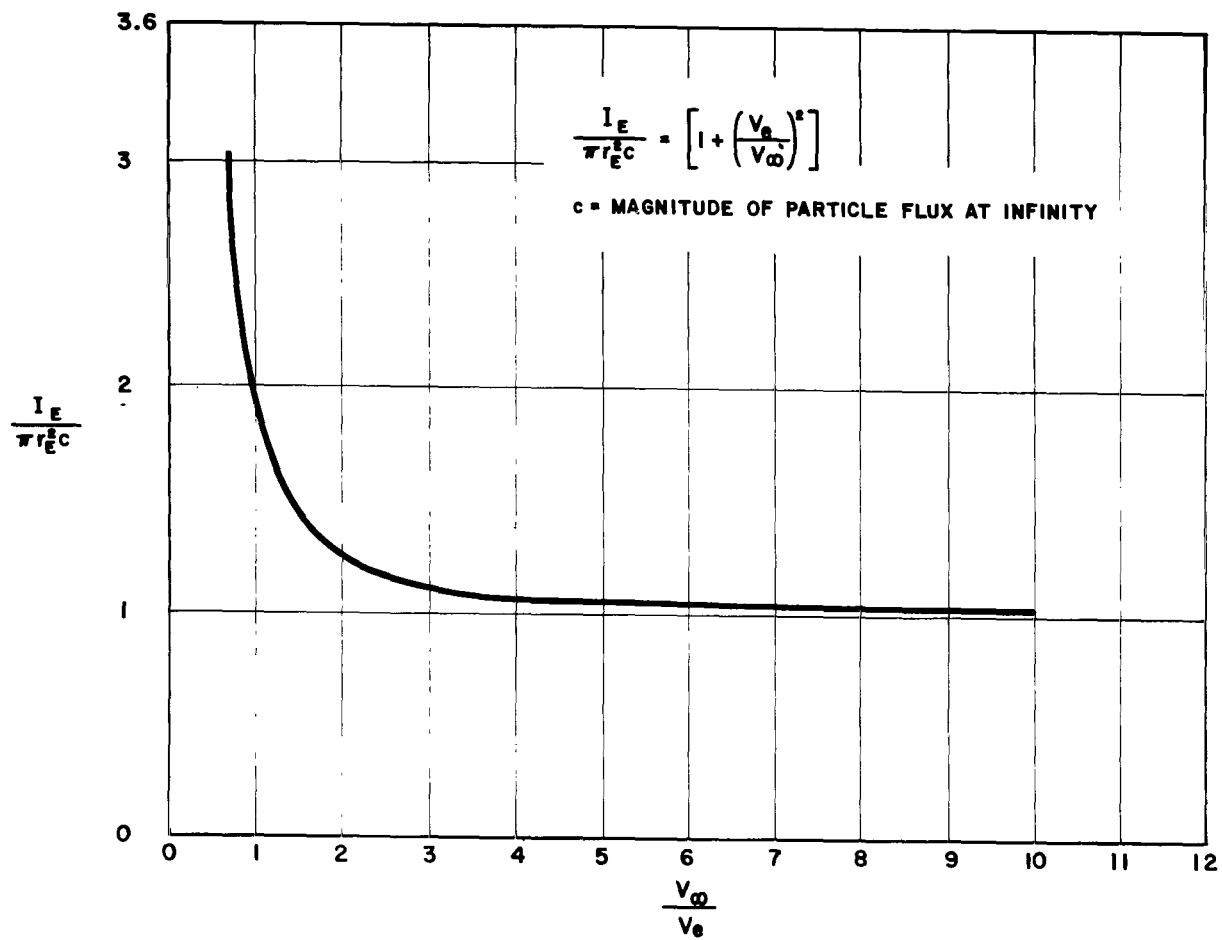


FIGURE 7. RELATIVE NUMBER OF PARTICLES INTERCEPTED BY THE EARTH AS A FUNCTION OF METEOROID VELOCITY AT INFINITY

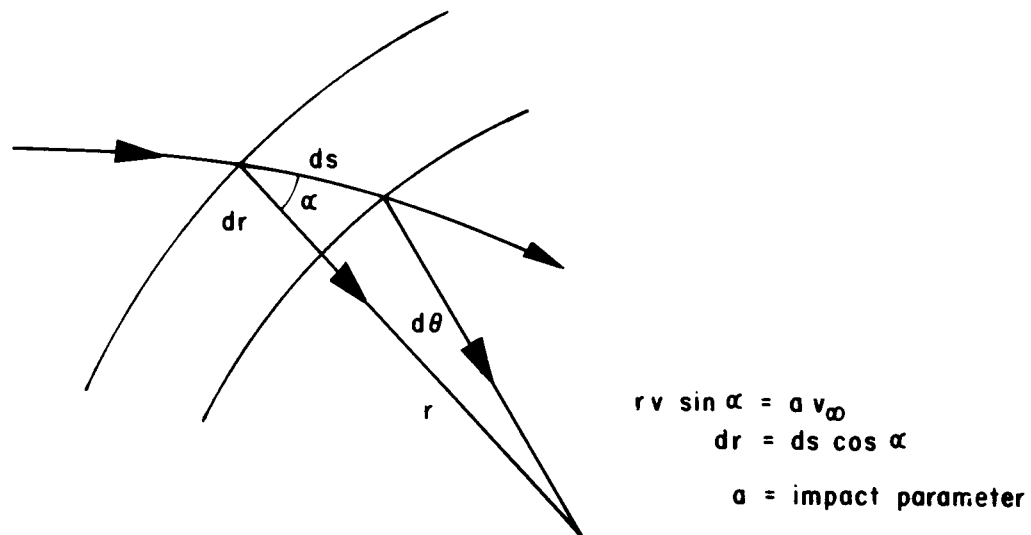


FIGURE 8. THE RELATIONSHIP OF THE ELEMENT OF TRACK LENGTH ds TO THE CONSERVATION OF ANGULAR MOMENTUM

The path length contributed by particles with impact parameters between a and $a + da$ is given by

$$4\pi a da ds c = 4\pi a c da dr / \left[1 - (av_{\infty}/rv)^2 \right]^{1/2} \quad (53)$$

The total path length in the differential element of volume $4\pi r^2 dr$ is found by integrating this expression with respect to a and subtracting the part which intersects the earth. The average flux $\langle \phi \rangle$ over the surface is this integral divided by $4\pi r^2 dr$, viz.

$$\begin{aligned} \langle \phi \rangle = & \left\{ \int_{a=0}^{a=a} 4\pi a c da dr / \left[1 - (av_{\infty}/rv)^2 \right]^{1/2} \right. \\ & \left. - \int_{a=0}^{a=a_E} 2\pi a c da dr / \left[1 - (av_{\infty}/rv)^2 \right]^{1/2} \right\} / 4\pi r^2 dr \end{aligned} \quad (54)$$

or, since the flux at infinity is equal to c ,

$$\begin{aligned} \langle \phi \rangle / \phi_{\infty} = & \frac{1}{r^2} \left\{ \int_{a=a_E}^{a=a} a da / \left[1 - (av_{\infty}/rv)^2 \right]^{1/2} \right. \\ & \left. + \frac{1}{2} \int_{a=0}^{a=a_E} a da / \left[1 - (av_{\infty}/rv)^2 \right]^{1/2} \right\} \end{aligned} \quad (55)$$

where, from Equation 43,

$$a = vr/v_{\infty} \quad (56)$$

$$a_E = v_E r_E / v_{\infty} \quad (57)$$

and

$$\int a da / \left[1 - \left(\frac{a v_{\infty}}{rv} \right)^2 \right]^{1/2} = - \left(\frac{rv}{v_{\infty}} \right)^2 \left[1 - (av_{\infty}/rv)^2 \right]^{1/2} \quad (58)$$

Therefore,

$$\langle \phi \rangle / \phi(\infty) = \frac{1}{2} \left(\frac{v}{v_\infty} \right)^2 \left\{ 1 + \left[1 - \left(\frac{r_E^{VE}}{rv} \right)^2 \right]^{1/2} \right\} \quad (59)$$

This is the same result as for the isotropic case, as expected.

A. STRUCTURE OF THE FLUX FIELD FOR THE MONOENERGETIC, MONO-DIRECTIONAL CASE

1. Basic Trajectory Geometry and Perspective. Consider the physical situation represented in Figure 6 wherein a very broad stream of particles, mono-directional and monoenergetic at infinity, is incident upon a sphere of radius, r , centered about the source of an attractive inverse square central force field. We begin our analysis by considering a very thin filament of the stream, and we recognize by virtue of the axial symmetry of the distribution depicted in Figure 6 that the behavior of this filament is typical of a set of trajectories which form the elements of a cylindrical shell at infinity.

Let $J(\infty)$ represent the magnitude of the flux vector at infinity; and let "a" be the value of the impact parameter which characterizes all of the trajectories forming a cylindrical shell of radius "a". At a point in the vicinity of the center of force, the flux vector will be denoted by $J(\bar{r})$. In particular, consider the particle current crossing a unit area of the sphere about the attractive center. The trajectories composing this current are characterized by some value "a" of the impact parameter. If $d\bar{A}$ is the elemental area, and α the angle between $\bar{J}(\bar{r})$ and $-d\bar{A}$, as shown in Figure 9, this current is

$$-\bar{J}(\bar{r}) \cdot d\bar{A} = J(\bar{r}) dA \cos \alpha = 2\pi a da J(\infty). \quad (60)$$

Writing the element of area dA in spherical coordinates as

$$dA = 2\pi r^2 \sin \theta d\theta \quad (61)$$

we have after rearrangement,

$$J(\bar{r})/J(\infty) = \frac{a da}{r^2 \sin \theta \cos \alpha d\theta} \quad (62)$$

where α is the angle between a trajectory tangent vector and the radius vector \bar{r} at the point where the trajectory intersects the sphere of radius, r .

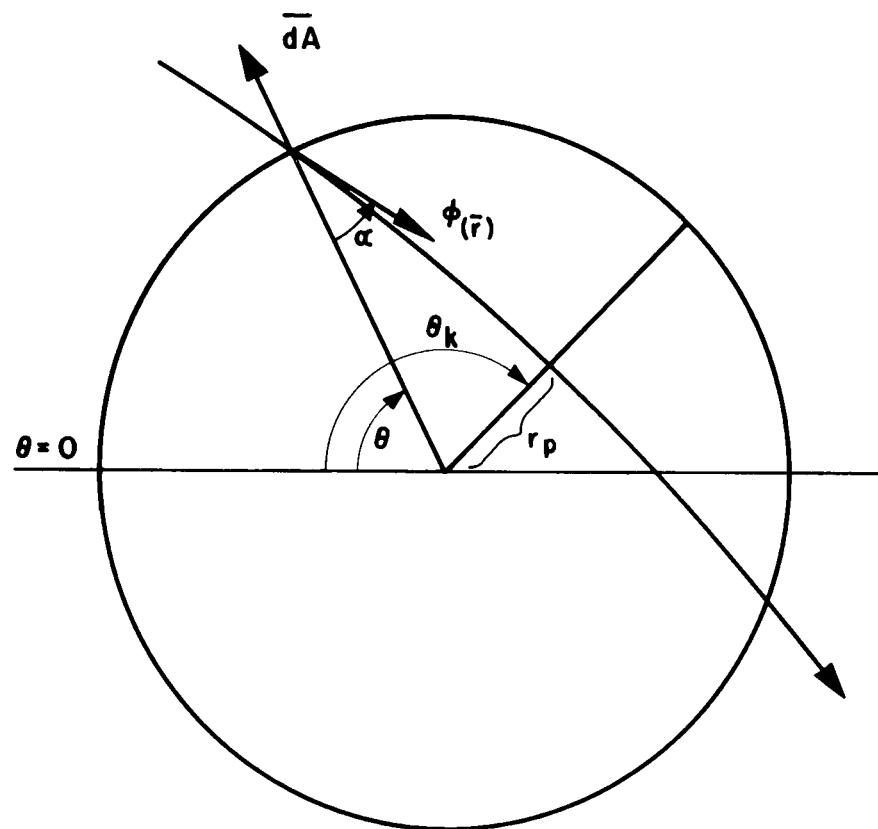


FIGURE 9. PERIGEE AND BASIC ANGLES

From Equation 50 and Figure 8,

$$\sin \alpha = \frac{v_{\infty} a}{r v(r)} = \frac{a v_{\infty}}{r [v_{\infty}^2 + 2\gamma M/r]^{1/2}} = \frac{a}{r [1 + 2/\gamma y]^{1/2}} \quad (63)$$

where we have related the velocities at r and at infinity by means of Equation 6, and have introduced an inverse distance

$$y \equiv \frac{v_{\infty}^2}{\gamma M} \quad (64)$$

From Equations 63 and 64

$$\begin{aligned} \cos \alpha &= + (1 - \sin^2 \alpha)^{1/2} = \left[\frac{y^2 r^2 + 2\gamma y - y^2 a^2}{y^2 r^2 + 2\gamma r} \right]^{1/2} \\ &= \left[\frac{y^2 r^2 + 2\gamma y - y^2 a^2}{y^2 r^2 + 2\gamma y} \right]^{1/2} \end{aligned} \quad (65)$$

We postulate¹ that the trajectories are hyperbolae (unbound particles of the form

$$r = y a^2 / \left\{ 1 + [1 + y^2 a^2]^{1/2} \cos (\theta - \theta_k) \right\} \quad (66)$$

where the eccentricity ϵ is given by

$$\epsilon \equiv \sqrt{1 + y^2 a^2} \equiv \sqrt{1 + k} \quad (67)$$

By using the requirement that r must go to infinity as θ approaches zero, it is seen that

$$1 + \epsilon \cos (-\theta_k) = 0 \quad (68)$$

or

$$\cos \theta_k = -1/\epsilon \quad ;$$

$$\theta_k = \cos^{-1} (-1/\epsilon) = \cos^{-1} \left(\frac{-1}{\sqrt{1+k}} \right) \quad (69)$$

1. "The general equation of a conic." Goldstein, H., Classical Mechanics, Addison-Wesley, p. 78. 1959.

The trajectory is closest to the origin when $\theta = \theta_k$. This minimum r , or perigee r_p , occurs when the denominator of Equation 66 is maximum; i. e. when $\theta = \theta_k$; and

$$r_p = \frac{ya^2}{1 + \epsilon} . \quad (70)$$

The angle θ_k is a monotonic decreasing of k ; $k = 0$ corresponds to a trajectory whose perigee is at $\theta = \pi$, while very large k values correspond to θ_k but slightly larger than $\pi/2$.

Equation 66 can be regarded as the classical form

$$r = \frac{a'(\epsilon^2 - 1)}{1 + \epsilon \cos \phi} \quad (71)$$

in terms of which the theory of conics is usually discussed; " a' " is called the semi-transverse axis of the hyperbola. In our case $\epsilon > 1$, and with our choice for the $\theta = 0$ direction, namely, that direction anti-parallel to the incident stream at infinity, Equation 71 represents a pair of hyperbolae whose major branch (i. e., $r > 0$) has the force center as an internal focus.

We can now straightforwardly make the following geometrical identifications, and in so doing we point out that the significance of a given k value is that it selects a set of trajectories possessing in common, one focus, a line of symmetry ($\theta = \theta_k$), and the same asymptotes.

The half angle β between the asymptotes is given by

$$\tan \beta = \frac{a v_{\infty}^2}{\gamma M} = \sqrt{k} = ya . \quad (72)$$

Defining the distance between the perigee of any pair of hyperbolae (major branch and its conjugate) to be $2a'$, one finds that

$$a' = \frac{1}{y} = \frac{\gamma M}{v_{\infty}^2} \quad (73)$$

and

$$2\epsilon a' = 2\epsilon/y = \frac{2\sqrt{1+k}}{y}$$

is the distance between the source and the other focus for any pair of hyperbolae. These relationships are shown in Figure 10, where they are also displayed in terms of k and the impact parameter.

As energy varies at constant $k = y^2 a^2$, the distance at perigee and distance to the center all vary inversely by the same factor; this is not contrary to physical common sense (i. e., the greater the energy, the greater the perigee distance) because "a", the impact parameter is varying inversely with y . As either y is varied at a fixed impact parameter, or as "a", the impact parameter, is varied at constant energy y , one obtains a continuous spectrum of hyperbolae of monotonically varying θ_k and β_k . As y or "a" increases, θ_k decreases toward the limiting value of $\pi/2$, corresponding to a particle of infinite energy (hence undisturbed by the attractive center), or to a particle of infinite impact parameter (so far away that its trajectory is undeflected). Or to say the same thing another way, with either increasing energy or impact parameter, the axis of symmetry becomes perpendicular to \bar{v}_∞ ; and β , the half angle of the "cone" of trajectories increases toward $\pi/2$. For decreasing y or "a", "a" or y being held constant respectively, the cone of trajectories narrows and the axis of symmetry tends to become parallel to \bar{v}_∞ , resulting in greater and greater scattering angles.

2. The Flux Zones. Let us assume that observations of fluxes and currents are made on the surface of a sphere of a given radius, r . Once this radius is chosen, a selection has been made of that portion of the incident stream which can intersect the sphere. This establishes an upper limit, a_{\max} , for the impact parameter for any given y , in that trajectories possessing impact parameters greater than a_{\max} will not be affected enough by the attractive center to intersect the sphere. A lower limit a_{\min} is established for scattered "radiation" (particles that are crossing the surface of the sphere from the inside to the outside) by the finite radius of the earth. Those trajectories whose perigees are less than some r_A (in some sense a radius of the atmosphere) are terminated. Thus a spherical zone centered about the $\theta = 0$ line is screened from all scattered flux. Equation 45 immediately provides these limiting values of the impact parameters, viz.

$$a = r \left[1 + \frac{v_{er}^2}{v_\infty^2} \right]^{1/2} = r \left[1 + 2/ry \right]^{1/2} \begin{cases} a_{\max} = a(r) \\ a_{\min} = a(r_A) \end{cases} \quad (74)$$

where v_{er} is the magnitude of the escape velocity at the point located by \bar{r} .

We consider the flux to be composed of three components, of which one is called direct flux, ϕ_D , the other two being scattered fluxes, ϕ_S and ϕ'_S . At any point on the surface of the sphere of observation, flux approaching the earth (i. e. has yet to pass through perigee) is direct flux; flux receding from the earth (having attained perigee)

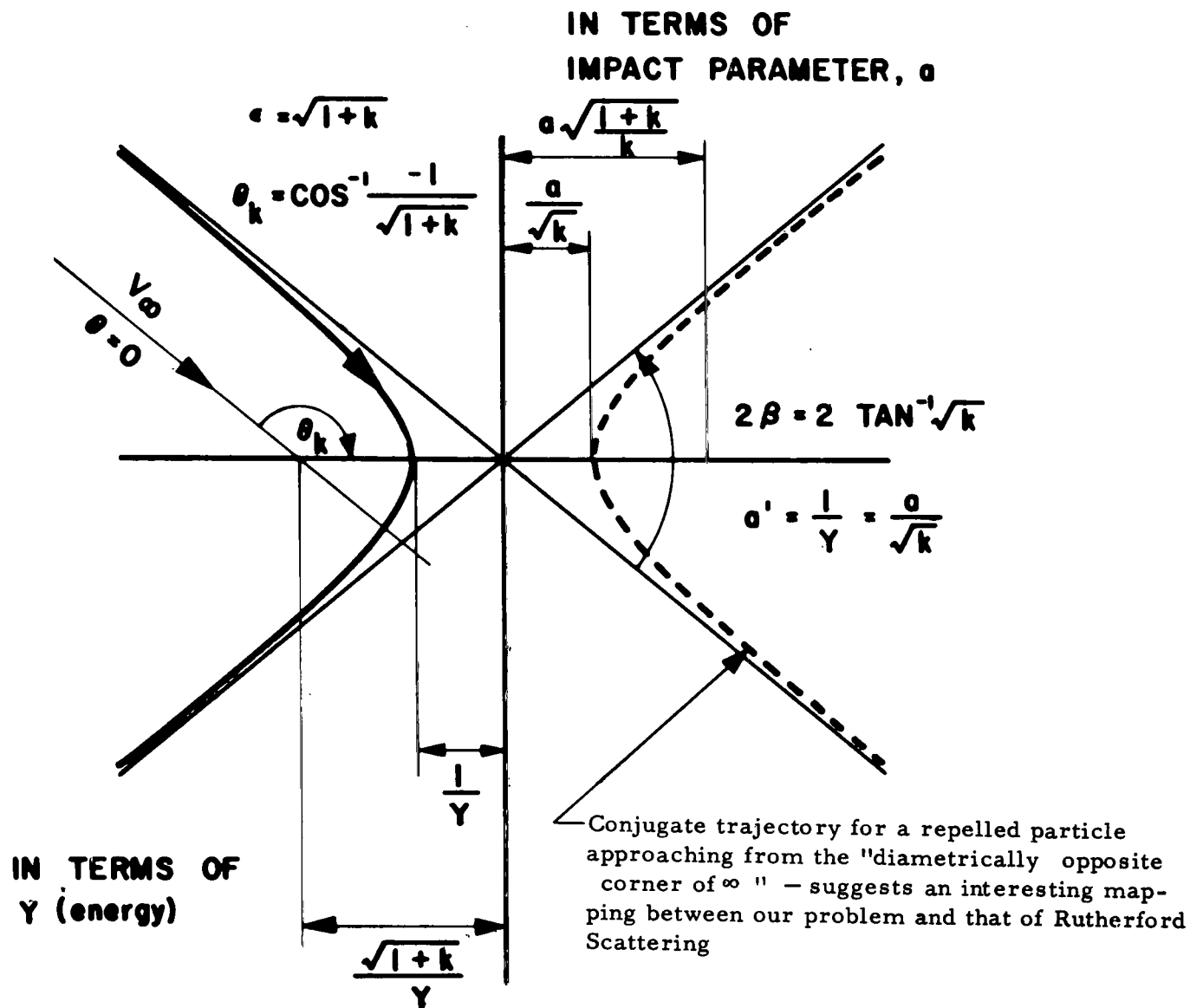


FIGURE 10. GEOMETRICAL IDENTIFICATION

is scattered flux. For purposes of mathematical convenience, scattered flux is considered to arise from two sources. Scattered flux, ϕ_S , arising from particles whose trajectories lie wholly in the same hemisphere¹, is distinguished from scattered flux, ϕ'_S , belonging to trajectories which penetrate both hemispheres. The zone, $0 < \theta < \pi$, defines the "upper hemisphere," the zone, $\pi < \theta < 2\pi$, defines the "lower hemisphere."

This classification of the fluxes divides the surface of the sphere of observation into zones as follows. For finite r_A , there is a zone, $0 \leq |\theta| \leq \theta_{\min}$ centered about $\theta = 0$ in which there is only direct flux where θ_{\min} is a function of y , r , and r_A .

Next, up to a direction specified by $\theta = \theta_{k \max}$ there is a zone upon which both scattered and direct flux, ϕ'_S and ϕ_D , are incident. For $|\theta| > \theta_{k \max}$ there can be only scattered fluxes, ϕ_S and ϕ'_S . There is a spherical sector defined by $|\theta| \leq \theta_\pi$ such that particles entering the sphere through this sector, all emerge from the other hemisphere; for $\theta_\pi < |\theta| < \theta_{k \max}$ all trajectories remain in the same hemisphere.

TABLE I

Summary of Flux Pattern in Upper Hemisphere

<u>Spherical Zone</u>	<u>Flux Components</u>	<u>Hemisphere in Which Direct Fluxes Emerge</u>
$0 < \theta \leq \theta_{\min}$	ϕ_D	intercepted by earth
$\theta_{\min} < \theta \leq \theta_\pi$	$\phi_D + \phi'_S$	lower
$\theta_\pi < \theta \leq \theta_{k \max}$	$\phi_D + \phi'_S$	upper
$\theta_{k \max} < \theta < \pi$	$\phi_S + \phi'_S$	no direct flux

The pattern in the lower hemisphere is the same because of symmetry. The zones and flux designations are shown in Figure 11.

At every point on the spherical surface we can now explicitly indicate the flux field in terms of the associated impact parameters (a_D and a_S or a'_S), their derivatives with respect to θ ; $\cos \alpha_D$, $\cos \alpha_S$, $\cos \alpha'_S$; $\sin \theta$ and $\cos \theta$, where the primes refer to quantities associated with the lower hemisphere. To arrive at a concision with readily comprehensible formulae, we must develop some elementary geometrical relationships between the θ 's and α 's and assume a convention for the latter.

1. Strictly semi-circles in the plane; however, "hemisphere" is conceptually helpful.

The convention on α will be that it is the angle from the inward pointing radius vector to the directed trajectory, defined to be positive in the counterclockwise sense. The trajectory is symmetric about the axis $\theta = \theta_k$; thus the geometry at exit is identical to the geometry at entry. Thus we can immediately write (See Fig. 12)

$$\alpha_S + \alpha_D = \pi \quad \alpha_S \text{ and } \alpha_D \geq 0 \text{ always .} \quad (75)$$

$$\alpha'_D + \alpha'_S = -\pi \quad \alpha'_D \text{ and } \alpha'_S \leq 0 \text{ always .} \quad (76)$$

where, as is the convention throughout, the prime refers to a trajectory entering the other (lower) hemisphere. These relations imply corresponding relationships between the impact parameters of the direct and scattered fluxes.

By the geometrical symmetry, for every trajectory the following relation holds between the angles made by the direct and scattered fluxes at their point of entry and exit from a sphere of observation:

$$\frac{\theta_D + \theta_S}{2} = \theta_k \quad (77)$$

If $\theta_D = \theta_k$ (i.e., grazing incidence), then $\theta_S = \theta_k$; if $\theta_S \equiv \theta_\pi$, then $\theta_D \equiv \theta_\pi = 2\theta_k - \pi$. Note the introduction of θ_π , the angle of entry such that the trajectory exits at $\theta = \pi$; there is an associated value for the impact parameter a_π which will be determined subsequently.

Because the earth possesses an atmosphere of finite radius r_A , effective in stopping meteoric particles, not all zones of a sphere of observation receive scattered flux. The impact parameter characterizing the limiting trajectory can be easily found by taking the perigee distance $r_p = r_A$ in Equation 70; thus

$$r_p = r_A = 1 + \frac{ya_{\min}^2}{\sqrt{1 + y^2 a_{\min}^2}} \quad (78)$$

Therefore,

$$a_{\min} = r_A (1 + 2/yr_A)^{1/2} \quad (79)$$

This value of "a" when substituted into the trajectory equation (Eq. 66) yields

$$\cos(\theta - \theta_{k\min}) = \frac{ya_{\min}^2 (r_A) - r}{r \epsilon(r_A)} \quad (80)$$

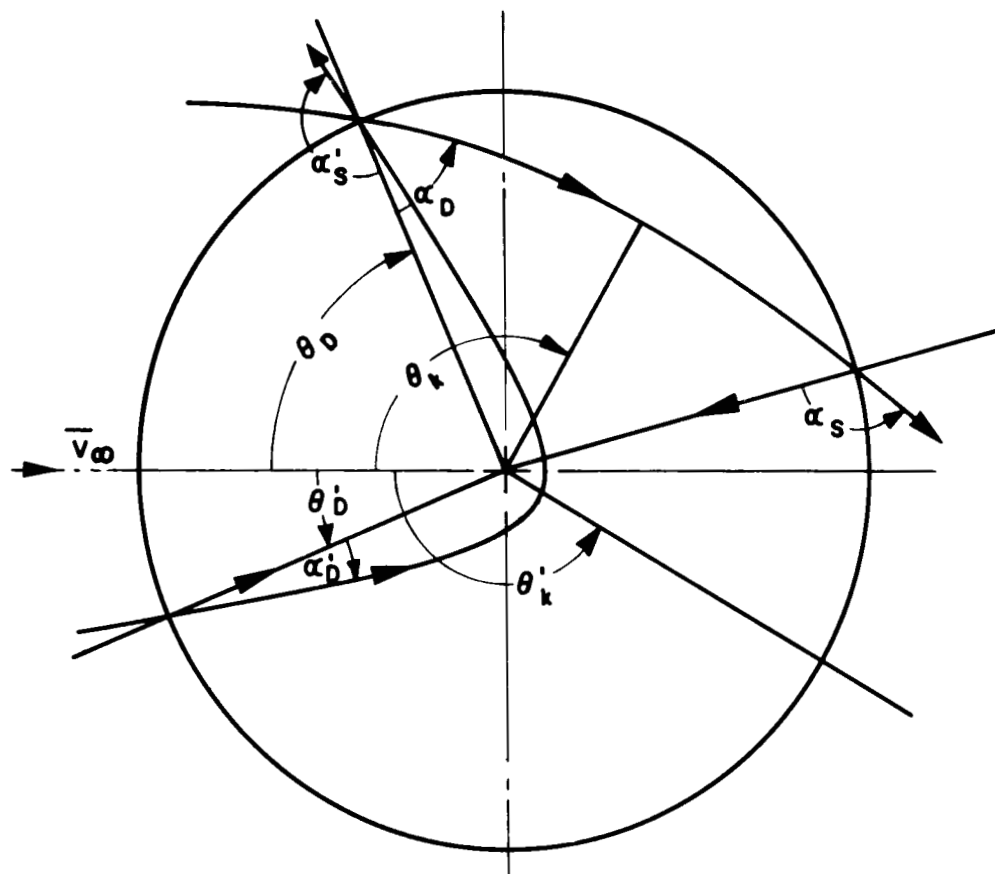


FIGURE 12. RELATIONS BETWEEN THE α 's

which is satisfied by two values of θ . The minimum angle θ_{\min} at which scattered flux can be received, is the angle of exit of the trajectory characterized by a_{\min} ; it is the larger of the two angles just determined. In order to refer our result to the upper hemisphere, we use 2π minus this angle instead of the angle itself.

A similar use of Equation 66, solving for impact parameter rather than for angle, and recalling that impact parameter appears in ϵ , yields

$$a_{\max} = r \sqrt{1 + \frac{2}{ry}}; \quad (81)$$

$$a_{\pi} = \sqrt{2r/y}. \quad (82)$$

where a_{\max} is the largest value of the impact parameter permitting a trajectory within a sphere of radius r ; and a_{π} is the impact parameter corresponding to that trajectory which exits from the sphere at $\theta = \pi$.

3. The Conjugate Trajectories. In the foregoing we have discussed direct and scattered fluxes without explicitly proving that, with the exception of a zone receiving only direct flux (an effect due to the earth not being a point mass), every field point is threaded by two trajectories, i. e., a direct and a scattered trajectory, or two scattered trajectories.

The trajectory equation for given r and θ is a quadratic equation determining two values for the impact parameter. Thus, using Equations 66 and 69,

$$a = \frac{ry \sin \theta \pm \sqrt{r^2 y^2 \sin^2 \theta + 4 ry(1 - \cos \theta)}}{2y} \quad (83)$$

Both values of "a" correspond to real trajectories. This is obvious for a positive¹ "a", henceforth denoted by a_+ ; that a_- , the negative value, also characterizes a trajectory, is evident from the following.

Let $a_- = -a'$ and substitute in the trajectory equation obtaining

$$r = \frac{ya'^2}{1 - \cos \theta - ya' \sin \theta} \quad (84)$$

which differs from our original equation by the sign preceding $ya' \sin \theta$ in the denominator. Next consider the transformation $\theta = -\theta'$ applied to the original trajectory equation.

1. a_{π} and a_{\max} of the preceding section are both on the positive branch of Equation 72.

Basically this amounts to changing the convention for positive θ from the clockwise to counterclockwise direction. The result is

$$\frac{ya^2}{1 - \cos \theta + ya \sin \theta} \rightarrow \frac{ya^2}{1 - \cos \theta' - ya \sin \theta'} \quad (85)$$

which shows Equation 84 does represent a hyperbola, in particular, one which is the reflection over the line $\theta = 0$, of

$$r = \frac{ya'^2}{1 - \cos \theta + ya' \sin \theta} \quad (86)$$

where "a'" may be $|a_-|$.

Thus, rewriting Equation 84 in terms of θ'

$$r = \frac{ya'^2}{1 - \cos \theta' + ya' \sin \theta'} \quad (87)$$

and we have recaptured the proper form. Evaluation of Equation 87 at the point (r, θ) in the upper hemisphere requires that θ' be replaced by $-\theta$ since the angles in Equation 87 are measured positive in the counterclockwise sense. One therefore has upon substituting $a = -a_-$ as well,

$$r = \frac{ya^2}{1 - \cos(-\theta) + ya' \sin(-\theta)} = \frac{ya_-^2}{1 - \cos \theta + ya_- \sin \theta} \quad (88)$$

which by definition is satisfied at (r, θ) .

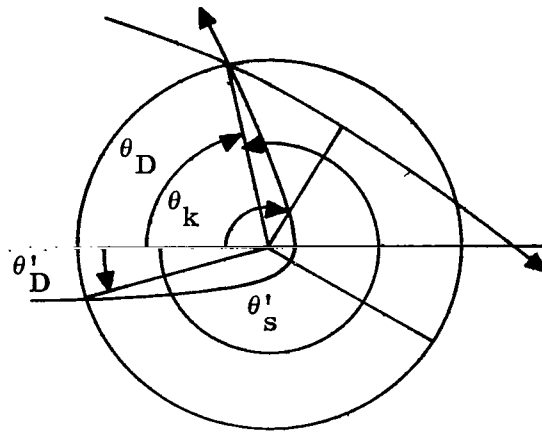
Next it is desirable to relate the angles of entrance and egress of the conjugate trajectories at any point, i. e., trajectories intersecting at that point. Corresponding to Equation 77 for any trajectory incident on the upper hemisphere.

$$\frac{\theta_D' + \theta_S'}{2} = \theta_k' \quad (89)$$

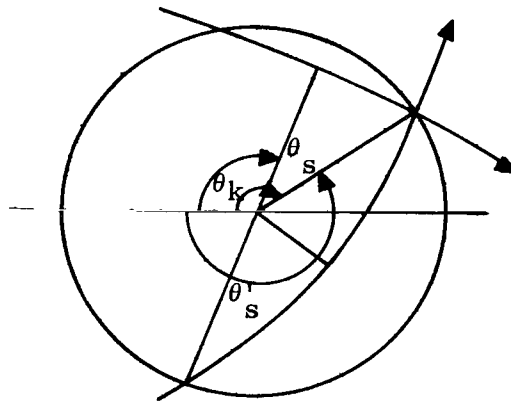
for the primed or conjugate trajectory. The connection between θ_D and θ_D' is immediately established by substituting (Fig. 13)

$$\theta_S' = \theta_D \quad (90)$$

for intersections at points where $\theta < \theta_{k \max}$. The resulting relation is



(a) INTERSECTION FOR $\theta < \theta_{k \max}$



(b) INTERSECTION FOR $\theta > \theta_{k \max}$

FIGURE 13. CONJUGATE TRAJECTORIES

$$\theta_D' + \theta_D = 2 \theta_k' , \quad (91)$$

$$\theta_D = \theta_S' < \theta_{k \max} .$$

If the intersection is that of scattered trajectories, i. e. , $\theta > \theta_{k \max}$ at the point of intersection, it is clear from Figure 13 that $\theta_S' = \theta_S$. Accordingly,

$$\frac{\theta_D' + \theta_S'}{2} = \theta_k' \text{ implies } \theta_D' + \theta_S = 2 \theta_k' , \quad (92)$$

and subtracting Equation 77, one finds

$$\begin{aligned} \theta_D - \theta_D' &= 2(\theta_k - \theta_k') , \\ \theta_S &= \theta_S' > \theta_{k \max} . \end{aligned} \quad (93)$$

Other interesting relationships can be readily derived; however, our aim here is merely to provide a foundation for further analysis and to introduce the concepts necessary for a succinct description of the flux field in the next section.

4. Exhibition of the Flux Field. In order to make a brief comprehensible presentation of the flux field, we rewrite the formulae for the basic parameters along with explanatory remarks.

The basic equation is Equation 62

$$J(r)/J_\infty = \frac{a}{r^2 \sin \theta \cos \alpha} \frac{da}{d\theta} \quad (94)$$

wherein all quantities have been previously introduced with the exception of $da/d\theta$.

From Equation 83

$$a = \frac{ry \sin \theta \pm \sqrt{r^2 y^2 \sin^2 \theta + 4 yr (1 - \cos \theta)}}{2y} \quad (95)$$

a_+ corresponds to contributions to direct flux upon entry of the trajectory, and to flux scattered in the same hemisphere (as it entered) upon exit of the trajectory; a_- corresponds to scattered flux that entered from the other (lower) hemisphere.

$$\frac{da}{d\theta} = \frac{1}{2} \left[r \cos \theta \pm \frac{(r^2 y \cos \theta \sin \theta + 2r \sin \theta)}{\sqrt{r^2 y^2 \sin^2 \theta + 4yr(1-\cos \theta)}} \right] \quad (96)$$

This derivative must be evaluated for the calculation of flux at a point; however, for applications involving integrations over the sphere's surface, the $d\theta$ can usually be divided out into the $d\theta$ of the surface element, to convert an integration over θ into a simpler one over impact parameter. The derivative $da/d\theta$ is positive for direct flux contributions and negative for scattered flux.

Finially, $\cos \alpha$ as derived in Equation 65, is for direct flux in the upper hemisphere. More generally

$$\cos \alpha_{\pm} = \pm \left[\frac{y^2 r^2 + 2yr - y^2 a_{\pm}^2}{y^2 r^2 + 2yr} \right]^{1/2} \quad (97)$$

where the \pm subscripts on α correlate with the sign in front of the brackets, and not with the choice made for "a" — i. e., a_+ or a_- . Of the various possibilities only the following are of immediate interest; the others correspond to symmetric trajectories describing identical situations in the lower hemisphere.

$$\begin{array}{ll} \text{For direct flux } \phi_D & a = a_+ \\ \alpha = \theta_D ; \theta < \alpha_D < \pi/2 ; 0 < \cos \alpha_D \equiv \cos \alpha_+ & \end{array} \quad (98)$$

$$\begin{array}{ll} \text{For scattered flux } \phi_S & a = a_+ \\ \alpha = \alpha_S = \pi - \alpha_D ; \pi/2 < \alpha_S ; \cos \alpha_S = - \cos \alpha_D = \cos \alpha_- & \end{array} \quad (99)$$

$$\begin{array}{ll} \text{For scattered flux } \phi'_S & a = a_- \\ \alpha = \alpha'_S = - \pi - \alpha'_D ; 0 < -\alpha'_D < \pi/2 ; \text{ so, } 0 > \cos \alpha'_S = \cos \alpha_- & \end{array}$$

$$\pi/2 < -\alpha'_S \quad (100)$$

where α'_D refers to direct flux incident in the lower hemisphere. These relationships can be directly obtained from Figure 12 if one keeps in mind our convention on the sign of α .

This development permits one to consider any individual flux component contribution — e.g., ϕ_D , ϕ_S , and ϕ'_S , or components in any given direction, such as tangential and radial flux currents as they would be encountered by a detector.

Thus the inward radial flux is given by

$$J(\bar{r}, \hat{r}) = \phi_D \cos \alpha$$

and the counterclockwise tangential component by

$$J(\bar{r}, -\hat{\theta}) = \phi'_S \left| \sin \alpha'_D \right|$$

where $\hat{\theta}$ is the unit vector normal to r . To calculate the flux as it would be measured by a moving detector, one must apply the formulae from the later section on detector motion to these results, which are valid only for a detector at rest with respect to the attractive center.

Finally, in considering the total flux at a point we must add the magnitudes of the various contributions since the scattered and direct radiations are assumed incoherent.

Thus,

$$\underline{0 < \theta < \theta_{\min}} \quad ; \quad \phi(r, \theta) = \phi_D = \frac{a_+}{r^2 \sin \theta \cos \alpha_+} \frac{da_+}{d\theta}$$

$$\underline{\theta_{\min} < \theta < \theta_{k \max}} \quad ; \quad \phi = \phi_D + \left| \phi'_S \right|;$$

$$\phi_D = \frac{a_+}{r^2 \sin \theta \cos \alpha_+} \frac{da_+}{d\theta} ; \quad \phi'_S = \frac{+a_-}{+r^2 \sin \theta \cos \alpha_-} \left(\frac{da_-}{d\theta} \right)$$

$$\underline{\theta_{k \max} < \theta < \pi} \quad ; \quad \left| \phi \right| = \left| \phi_S \right| + \left| \phi'_S \right|$$

$$\phi_S = \frac{-a_+}{r^2 \sin \theta \cos \alpha_-} \left(\frac{da_+}{d\theta} \right)$$

$$\phi'_S = \frac{+a_-}{r^2 \sin \theta \cos \alpha_-} \left(\frac{da_-}{d\theta} \right)$$

(101)

where in $da +/d\theta$ the $+$ identifies the sign to be taken in evaluating Equation 96. Under the conventions we have assumed, a flux contribution is inherently positive if particles are entering the sphere of observation, and negative if it corresponds to departing radiation.

B. VERIFICATION BY DIRECT CALCULATION OF THE RESULT OBTAINED FROM THE APPLICATION OF LIOUVILLE'S THEOREM TO MONOENERGETIC ISOTROPIC DISTRIBUTIONS

In this section the formulae of the preceding discussion which were obtained for the monodirectional case, will be integrated over the surface of the sphere of observation to obtain averaged values of the direct and scattered fluxes. These will be simply combined by adding their magnitudes, since the radiation is assumed incoherent, and their sum will be identified with the radial distribution of flux obtained in the second section of this paper, thus, for the isotropic case, obtaining independently the result, that the radial dependence of the flux is as

$$\langle \phi(r) \rangle / \phi(\infty) = \left[\frac{v(r)}{v_\infty} \right]^2 = 1 + \frac{2}{ry} \quad (102)$$

We shall ignore the same effect due to the finite size of the scattering center. At each point there are two flux contributions, as has been discussed in detail. In developing these integrals, we shall rely heavily on the previous development and on Figure 11.

We desire

$$\left\langle \frac{\phi_r}{\phi_\infty} \right\rangle = \frac{\iiint \phi(r) dA}{\iiint dA} = \frac{\iiint \phi(r) dA}{4\pi r^2} \quad (103)$$

The θ integration is the only one of a non-trivial nature, and whatever difficulties this might entail we avoid entirely by converting the integrals to ones over impact parameter rather than angle. The flux $\phi(r)$ assumes different forms for the two major regions in the upper hemisphere, viz $0 < \theta < \theta_{k \max}$ where there is direct and scattered flux; and $\theta_{k \max} < \theta < \pi$ where there are scattered fluxes only.

$$\left\langle \frac{\phi_r}{\phi_\infty} \right\rangle = \int_0^\pi \phi(r) \sin \theta d\theta \quad (104)$$

where

$$\phi(r) = \begin{cases} |\phi_D| + |\phi'_S| & \theta \leq \theta_{k \max} \\ |\phi'_S| + |\phi_S| & \theta_{k \max} < \theta < \pi \end{cases} ; \quad (105)$$

Thus

$$\int_0^\pi \phi(r) \sin \theta d\theta = \int_0^{\theta_{k \max}} \{ |\phi_D| + |\phi'_S| \} \sin \theta d\theta + \int_{\theta_{k \max}}^\pi \{ |\phi_S| + |\phi'_S| \} \sin \theta d\theta \quad (106)$$

where ϕ_D , ϕ'_S , and ϕ_S are given by Equation 101. They are functions of a_\pm , $\cos \alpha_\pm$, and $da_\pm/d\theta$ specified by Equations 95 through 100 — altogether an unfriendly integral. In principle one could substitute these functions and straightforwardly perform the integration over θ . However, this we avoid by noticing that all integrations can be done over impact parameter — for, $(da/d\theta)d\theta$ is common to all integrands. Furthermore, since we are interested only in total contributions, the separation into components as indicated by Equation 104 is not necessary and indeed is not the most advantageous representation.

Expressing the integrals in terms of impact parameter

$$\begin{aligned} r^2 \int_0^{\theta_{k \max}} \phi_D \sin \theta d\theta &\rightarrow \int_0^{a_{\max}} \frac{a_+ da_+}{\cos \alpha_+} \\ r^2 \int_0^{\theta_{k \max}} \phi'_S \sin \theta d\theta + r^2 \int_{\theta_{k \max}}^\pi \phi'_S \sin \theta d\theta &= \\ r^2 \int_0^\pi \phi'_S \sin \theta d\theta &\rightarrow \int_0^\pi \frac{a_- da_-}{\cos \alpha_-} \end{aligned}$$

since all ϕ'_S contribution arises from conjugate trajectories entering the lower hemisphere at angles from 0 to $-\theta_\pi$ (see Eq. 77 et sequens).

$$r^2 \int_{\theta_{k \max}}^\pi \phi_S \sin \theta d\theta = r^2 \int_{\theta_\pi}^{\theta_{k \max}} \phi_S \sin \theta d\theta \rightarrow \int_{a_\pi}^{a_{\max}} \frac{a_+ da_+}{\cos \alpha_+}$$

since the total ϕ_S contribution enters the sphere as direct flux precipitating in the region $\theta_\pi < \theta < \theta_{k \max}$.

Now it is obvious that the \pm subscripts are meaningless (i.e., the a 's are dummy variables). Therefore, recognizing that $\cos \alpha_+$ and $\cos \alpha_-$ have the same functional dependence on a_- , we can write

$$r^2 \int_0^\pi \phi \sin \theta \, d\theta = \left[\int_0^{a_{\max}} \frac{a \, da}{\cos \alpha} + \int_0^{-a_\pi} \frac{a \, da}{\cos \alpha} + \int_{a_\pi}^{a_{\max}} \frac{a \, da}{\cos \alpha} \right] \quad (107)$$

Since we are concerned only with magnitudes, we may replace

$$\int_0^{-a_\pi} \frac{a \, da}{\cos \alpha} \text{ by } \int_0^{a_\pi} \frac{a \, da}{\cos \alpha} \text{ since in this example, } \int_0^{-a} = - \int_0^a$$

Then

$$\int_0^\pi \phi_r \sin \theta \, d\theta = \frac{1}{r^2} \left\{ \int_0^{a_{\max}} \frac{a \, da}{\cos \alpha} + \int_0^{a_{\max}} \frac{a \, da}{\cos \alpha} \right\}$$

or

$$\int_0^\pi \phi_r \sin \theta \, d\theta = \frac{2}{r^2} \int_0^{a_{\max}} \sqrt{\frac{a \, da}{\frac{y^2 r^2 + 2yr - y^2 a^2}{y^2 r^2 + 2yr}}} \quad (108)$$

Finally, from Equation 106

$$\begin{aligned} \left\langle \frac{\phi_r}{\phi_\infty} \right\rangle &= \frac{(y^2 r^2 + 2yr)^{1/2}}{-r^2 y^2} \int_0^{a_{\max}} \frac{-2y^2 a \, da}{(y^2 r^2 + 2yr - y^2 a^2)^{1/2}} \\ &= \frac{(y^2 r^2 + 2yr)^{1/2}}{r^2 y^2} \left. (y^2 r^2 + 2yr - y^2 a^2)^{1/2} \right|_{a_{\max}}^0 = \\ &= \frac{(y^2 r^2 + 2yr) - (y^2 r^2 + 2yr)^{1/2} [y^2 r^2 + 2yr - (y^2 r^2 + 2yr)]}{r^2 y^2} \end{aligned} \quad (109)$$

where from Equation 74

$$a_{\max} = r \left(1 + \frac{2}{ry} \right)^{1/2}, \text{ all reducing to}$$

$$\left\langle \frac{\phi(r)}{\phi_{\infty}} \right\rangle = \frac{y^2 r^2 + 2yr}{y^2 r^2} = \left(1 + \frac{2}{ry} \right)$$

in full agreement with Equation 20, the Liouville theorem result.

Or, substituting $y = \frac{v_{\infty}^2}{\gamma M}$ and recalling Equation 6

$$\left\langle \frac{\phi_r}{\phi_{\infty}} \right\rangle = 1 + \frac{2}{yr} = \frac{a_{\max}^2}{r^2} = 1 + \frac{2\gamma M}{rv_{\infty}^2} = \left(\frac{vr}{v_{\infty}} \right)^2 \quad (110)$$

C. EFFECT OF DETECTOR MOTION ON IMPACT RATE

The motion of a particle detector changes both the energy and the direction of particle impact. Anyone who has ridden in a car at night during a snowstorm knows that, as the car gains speed, the snowflakes appear to arrive more and more rapidly from the forward direction. If we measure the rate of meteoroid impact from a moving satellite, we must know how to correct for the effect of satellite motion on the count rate and how to compute the increased penetration hazard faced by a vehicle because of its motion through space.

For purposes of computation, let us assume that we have two coordinate systems, one in which the radiation distribution function $N(\bar{r}, \bar{v})$ is to be determined. As shown in Figure 14, a particle is located in the first system by a position vector \bar{r} and in the second by a position vector \bar{r}' . The vector \bar{R} locates the second system relative to the first. By vector algebra

$$\bar{r} = \bar{R} + \bar{r}', \quad (111)$$

and by time differentiation

$$\bar{v} = \bar{V} + \bar{v}'. \quad (112)$$

In the following discussion, we will assume that R is zero but that \bar{V} is not, so that

$$\bar{r} = \bar{r}' \quad (113)$$

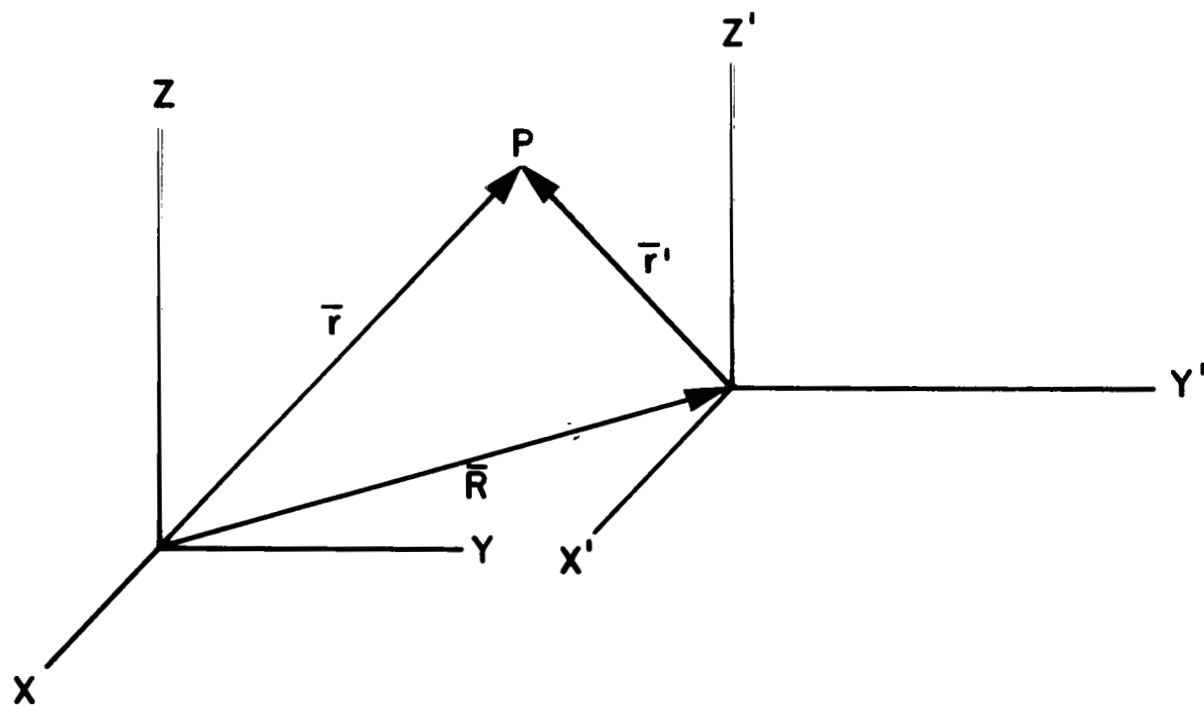


FIGURE 14. TRANSFORMATION OF SPATIAL COORDINATES

By performing the scalar product of each side of Equation 112 with itself, we obtain

$$v^2 = V^2 + v'^2 + 2 V v' \cos \theta' \quad (114)$$

Transposing \overline{V} in Equation 112 and repeating the operation, we obtain

$$v'^2 = v^2 + V^2 - 2Vv \cos \theta \quad (115)$$

The angles θ and θ' are as shown in Figure 15. These equations relate the kinetic energy of a particle in one system to its kinetic energy in the other. Furthermore, they are easily solved to obtain the speeds and directions observed in one system (v' , θ') in terms of their unprimed analogues (v , θ).

From Equation 114, we have

$$\cos \theta' = \frac{v^2 - v'^2 - V^2}{2v' V} ;$$

and substitution for v'^2 from Equation 115, followed by defining $z = \frac{v}{V}$ (shown as $z = \frac{v_0}{V}$ in the figures simply to avoid confusion), yields

$$\cos \theta' = \frac{z \cos \theta - 1}{\sqrt{z^2 + 1 - 2 z \cos \theta}} \quad (116)$$

This relationship is shown in Figure 16 for several z values.

In the primed system, the speed of a particle described by $v_0(v, \theta)$ in the unprimed system, results by solving Equation 114, which is a quadratic in v' . One finds

$$\frac{v'}{V} = \sqrt{z^2 + \cos^2 \theta' - 1 - \cos \theta'} \quad (117)$$

where $z = \frac{v_0}{V}$ as before, and we have taken the positive root — the negative v' not being required in our development. One could substitute $\cos \theta'$ from Equation 116 to obtain the relation between z and $z' \equiv \frac{v'}{V}$; however, this is not necessary for our purposes. Equation 117 is plotted in Figure 17 for the same z values used in Figure 16. One notices in the region $z < 1$ that for a given θ' and fixed z there are two solutions for v_0 and θ ; an associated double valuelessness exists in Figure 17.

In relating the distribution function $N(\bar{r}, \bar{v})$ and $N'(\bar{r}', \bar{v}')$, it is convenient to choose coordinate systems in such a way that the position vector \bar{r} and the azimuthal angle ϕ are unchanged by the coordinate transformations. These conditions are met in Equation 113. Because of the invariancy of the particle density to Galilean transformations

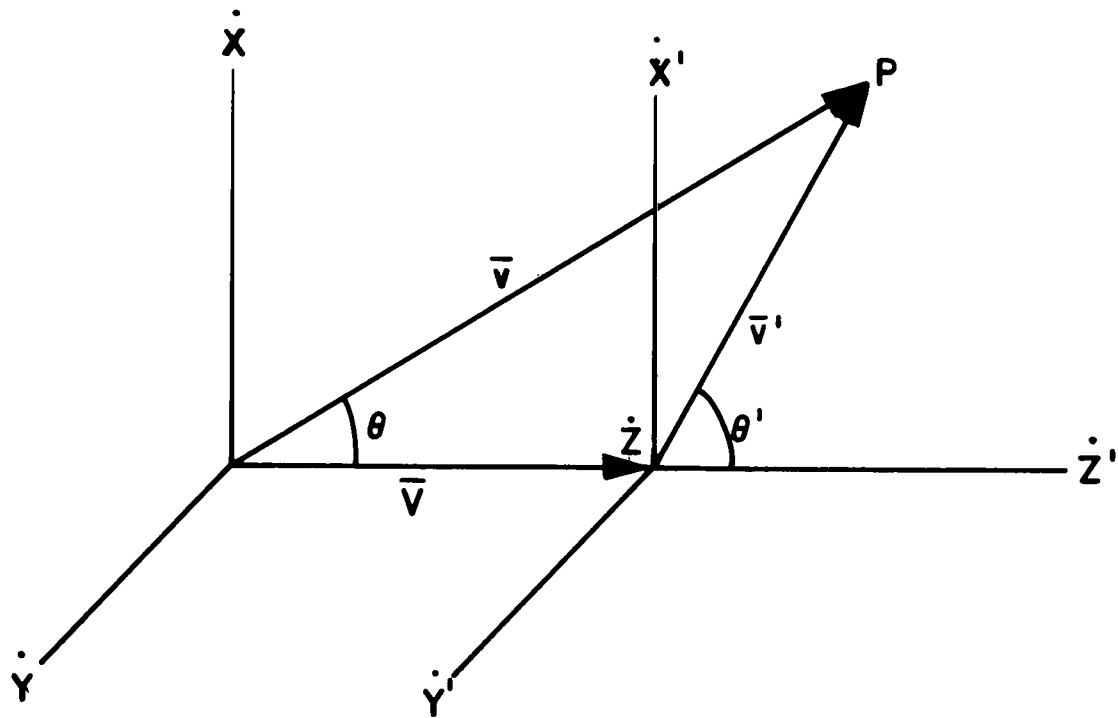


FIGURE 15. TRANSFORMATION OF VELOCITY COORDINATES

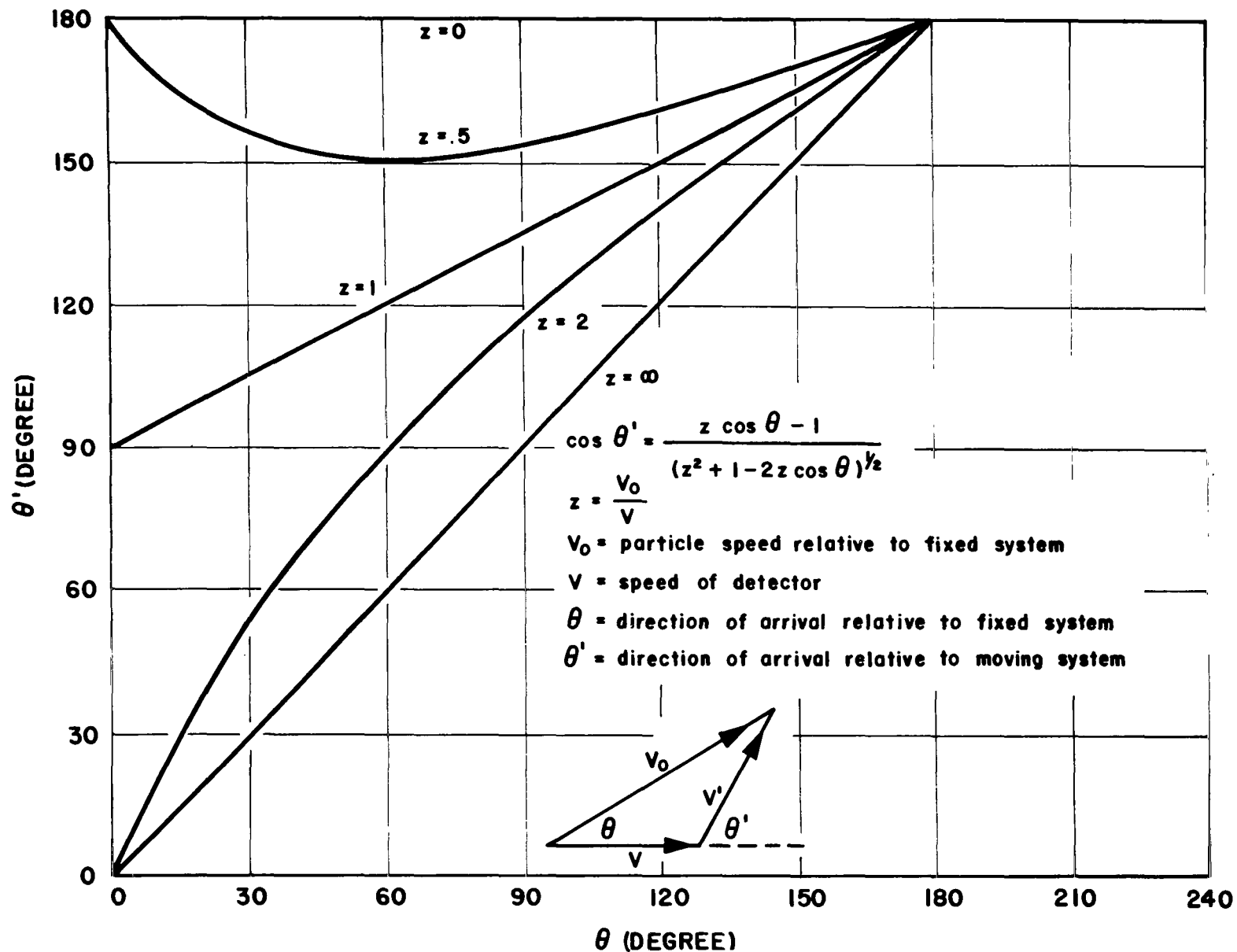


FIGURE 16. THE EFFECT OF DETECTOR MOTION ON DIRECTION OF ARRIVAL OF METEORIODS

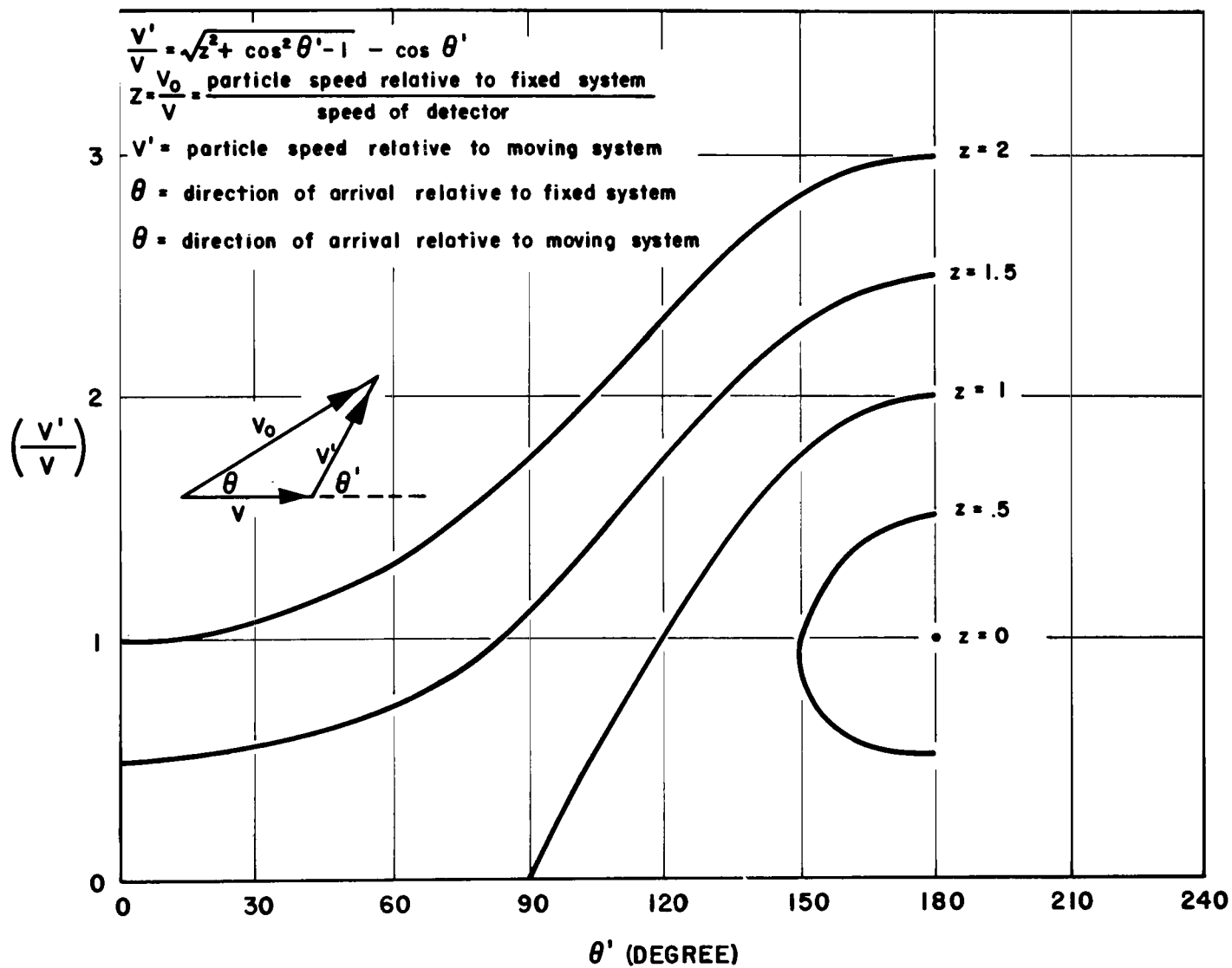


FIGURE 17. THE EFFECT OF DETECTOR MOTION ON IMPACT SPEED OF METEORIODS

$$N(\bar{r}) = \iiint_R N(\bar{r}, \bar{v}) d\bar{v} = \iiint_{R'} N'(\bar{r}', \bar{v}') d\bar{v}' = N'(\bar{r}') \quad (118)$$

By using the special conditions on our coordinate systems and the substitutions

$$\mu = \cos \theta, \quad \mu' = \cos \theta' \quad (119)$$

we can write the equation for particle density more explicitly as

$$\iiint_R N(\bar{r}, v, \phi) v^2 dv d\mu d\phi = \iiint_{R'} N'(\bar{r}, \bar{v}', \mu', \phi) v'^2 dv' d\mu' d\phi. \quad (120)$$

Transforming this last integral over the primed coordinates to the unprimed coordinates, one has

$$\begin{aligned} & \iiint_{R'} N'[\bar{r}, v', \mu', \phi] v'^2 dv' d\mu' d\phi = \\ & \iiint_R N'[\bar{r}, v'(v, \mu), \mu'(v, \mu), \phi] \frac{\partial(v' \mu')}{\partial(v \mu)} v'^2(v, \mu) dv d\mu d\phi \end{aligned} \quad (121)$$

or

$$\iiint_{R'} N'[\bar{r}, v', \mu', \phi] v'^2 dv' d\mu' d\phi = \iiint_R N'[\bar{r}, v'(v, \mu) \mu'(v, \mu) \phi] v^2 dv d\mu d\phi$$

where

$$\frac{\partial(v' \mu')}{\partial(v \mu)} = \frac{v^2}{v'^2} \quad (122)$$

is the Jacobian of the transformation¹ implied by Equations 114 and 115.

This result arises from the intrinsic properties of this transformation and is valid for any well behaved function of v' , μ' .

Thus any integral of the form

¹ Courant, Differential and Integral Calculus, p. 252.

$$f'(r) = \iiint_R f'[r, v', \mu', \phi] v'^2 dv' d\mu' d\phi \quad (123)$$

can be computed in terms of the unprimed coordinates by

$$f'(r) = \iiint_R f'[\bar{r}, v'(v, \mu), \mu'(v, \mu), \phi] v^2 dv d\mu d\phi \quad (124)$$

which may be more tractable.

Therefore expressing the integral over the primed coordinates in Equation 118 in terms of the unprimed coordinates,

$$\iiint N[\bar{r}, v, \mu, \phi] v^2 dv d\mu d\phi = \iiint N'[\bar{r}, v'(\mu v), \mu'(\mu v), \phi] v^2 dv d\mu d\phi, \quad (125)$$

since Equation 125 is valid for arbitrary pairs of associated regions R and R' one has

$$N[\bar{r}, v, \mu, \phi] v^2 = N'[\bar{r}, v'(\mu v), \mu'(\mu v), \phi] v^2$$

or

$$N[\bar{r}, v, \mu, \phi] = N'[\bar{r}, v'(\mu v), \mu'(\mu v), \phi] \quad (126)$$

For the particular case of uniform monoenergetic monodirectional radiation of speed v_0 ,

$$N(\bar{r}, v, \mu, \phi) = C \delta(v - v_0) \delta(\mu - \mu_0) \delta(\phi - \phi_0) \quad (127)$$

and the particle density $N(\bar{r})$ and flux $\phi(\bar{r})$ are given by

$$N(\bar{r}) = \iiint N(\bar{r}, v, \mu, \phi) v^2 dv d\mu d\phi = C v_0^2 \quad (128)$$

$$\phi(\bar{r}) = \iiint v N(\bar{r}, v, \mu, \phi) v^2 dv d\mu d\phi = C v_0^3 \quad (129)$$

In the other coordinate system, using Equations 115 and 125,

$$v' = \left[V^2 + v^2 - 2Vv\mu \right]^{1/2} \quad (130)$$

¹ A similar relation can be obtained by interchanging primed and unprimed variables.

and

$$\begin{aligned}\phi^*(r) &= \iiint \left[V^2 + v^2 - 2Vv\mu \right]^{1/2} C \delta(v - v_0) \delta(\mu - \mu_0) \delta(\phi - \phi_0) v^2 dv d\mu d\phi \\ &= C \left[V^2 + v_0^2 - 2Vv_0\mu_0 \right]^{1/2} v_0^2\end{aligned}\quad (131)$$

The ratio

$$\frac{\phi^*(\bar{r})}{\phi(\bar{r})} = \left[1 + \left(\frac{V}{v_0} \right)^2 - 2 \left(\frac{V}{v_0} \right) \mu_0 \right]^{1/2} \quad (132)$$

represents the multiplication factor for the flux as a function of detector motion. Figure 18 shows this effect for several values of V/v_0 and μ_0 . This result could of course have been obtained by more elementary means.

If the radiation is spatially uniform, monoenergetic, and isotropic, we can write

$$N(\bar{r}, \bar{v}) = C \delta(v - v_0) \quad (133)$$

The particle density $N(\bar{r})$ and flux $\phi(r)$ are given by

$$N(\bar{r}) = \iiint C \delta(v - v_0) v^2 dv d\mu d\phi = 4\pi C v_0^2 \quad (134)$$

$$\phi(\bar{r}) = \iiint C \delta(v - v_0) v^3 dv d\mu d\phi = 4\pi C v_0^3 \quad (135)$$

In the moving system, we are able to write, by the same reasoning as before, that

$$\phi^*(\bar{r}) = \iiint \left[v^2 + V^2 - 2Vv\mu \right]^{1/2} C \delta(v - v_0) v^2 dv d\mu d\phi \quad (136)$$

The integration over v , μ , and ϕ yields

$$\phi^*(r) = \frac{2\pi C V_0}{3V} \left[|v_0 + V|^3 - |v_0 - V|^3 \right] \quad (137)$$

The absolute value signs are used because v^* must always be positive. For $v_0 < V$, substituting Equation 135

$$\phi^*(r)/\phi(r) = (V/v_0 + v_0/3V) \quad (138)$$

and for $v_0 > V$

$$\phi^*(r)/\phi(r) = 1 + (1/3)(V/v_0)^2 \quad (139)$$

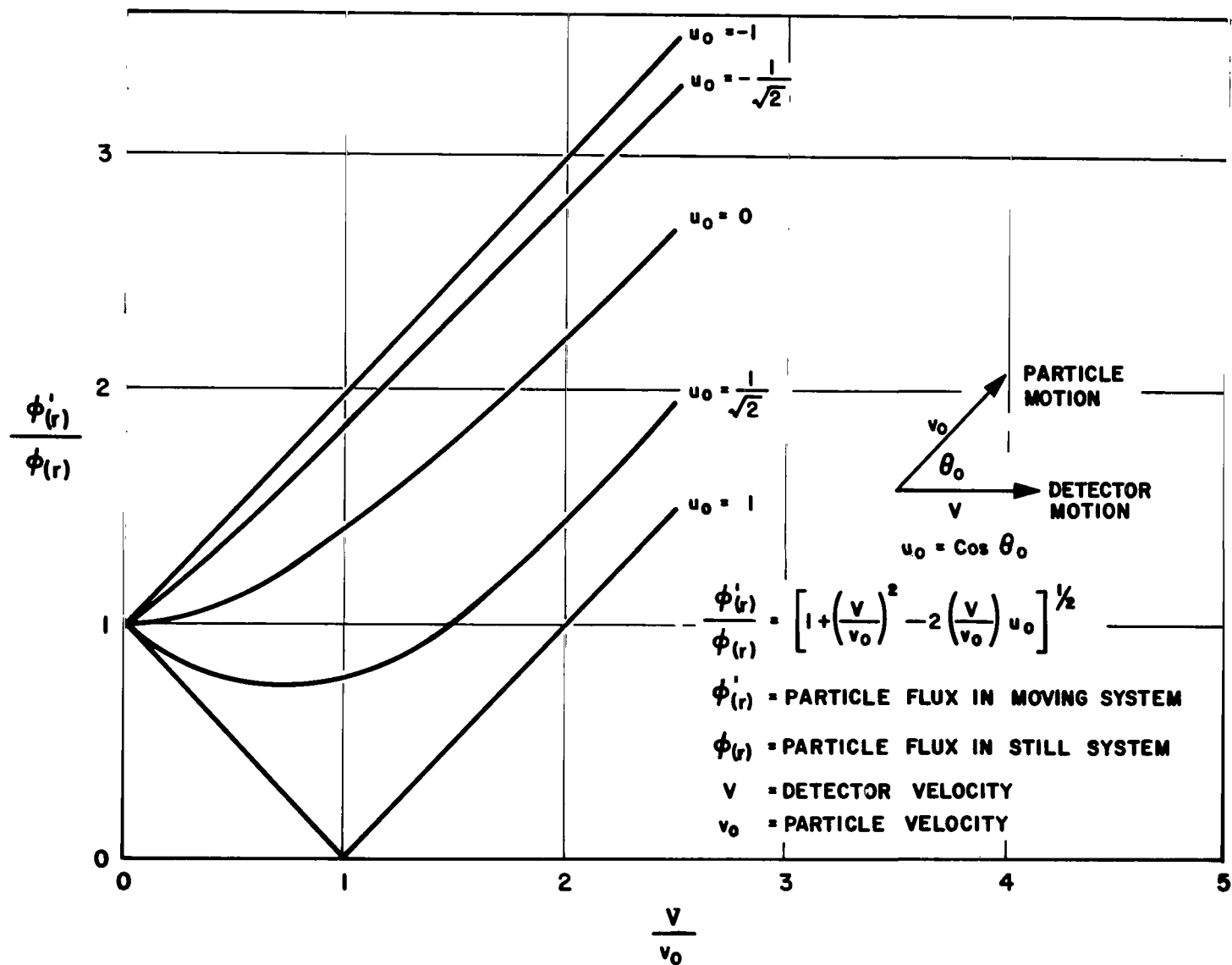


FIGURE 18. THE EFFECT OF DETECTOR MOTION ON A MONOENERGETIC, MONODIRECTIONAL FLUX

A graph of the effect of satellite motion on the isotropic monoenergetic particle flux is shown in Figure 19.

The total kinetic energy in the two systems is given by

$$\langle T \rangle = \frac{1}{2} m \iiint v^2 N(\bar{r}, \bar{v}) v^2 dv d\mu d\phi \quad (140)$$

$$\langle T' \rangle = \frac{1}{2} m \iiint v'^2 N(\bar{r}, \bar{v}) v^2 dv d\mu d\phi \quad (141)$$

For the monodirectional monoenergetic case, the ratio of Equations 140 and 141 is

$$\langle T' \rangle / \langle T \rangle = T' / T = 1 + \left(\frac{V}{v_0} \right)^2 - 2 \left(\frac{V}{v_0} \right) \mu_0 \quad (142)$$

For the isotropic monoenergetic case

$$\langle T' \rangle / \langle T \rangle = 1 + \left(\frac{V}{v_0} \right)^2 \quad (143)$$

Graphs of these functions are shown in Figures 20 and 21.

SECTION IV. CONCLUSIONS

The foregoing discussion has been in the form of a general survey to illustrate the magnitude and nature of some of the problems associated with measuring meteoroid flux from moving satellites. The application of the Liouville theorem represented an extension of a practice common to the treatment of charged particles in electromagnetic fields and the treatment of the structure of the flux field constituted an extension of the asymptotic discussion of the Rutherford scattering problem involving Coulomb repulsion to the region near an attracting force center. The problem of the orientation of a non-spherical detector was not considered.

An attempt will be made to apply the techniques developed here to the detailed interpretation of the count rate measured by the Saturn-boostered micrometeoroid satellite. Statistical methods must of course be developed to bridge the gap between the analytic streams assumed here and the paucity of counts expected from the coming experiment.

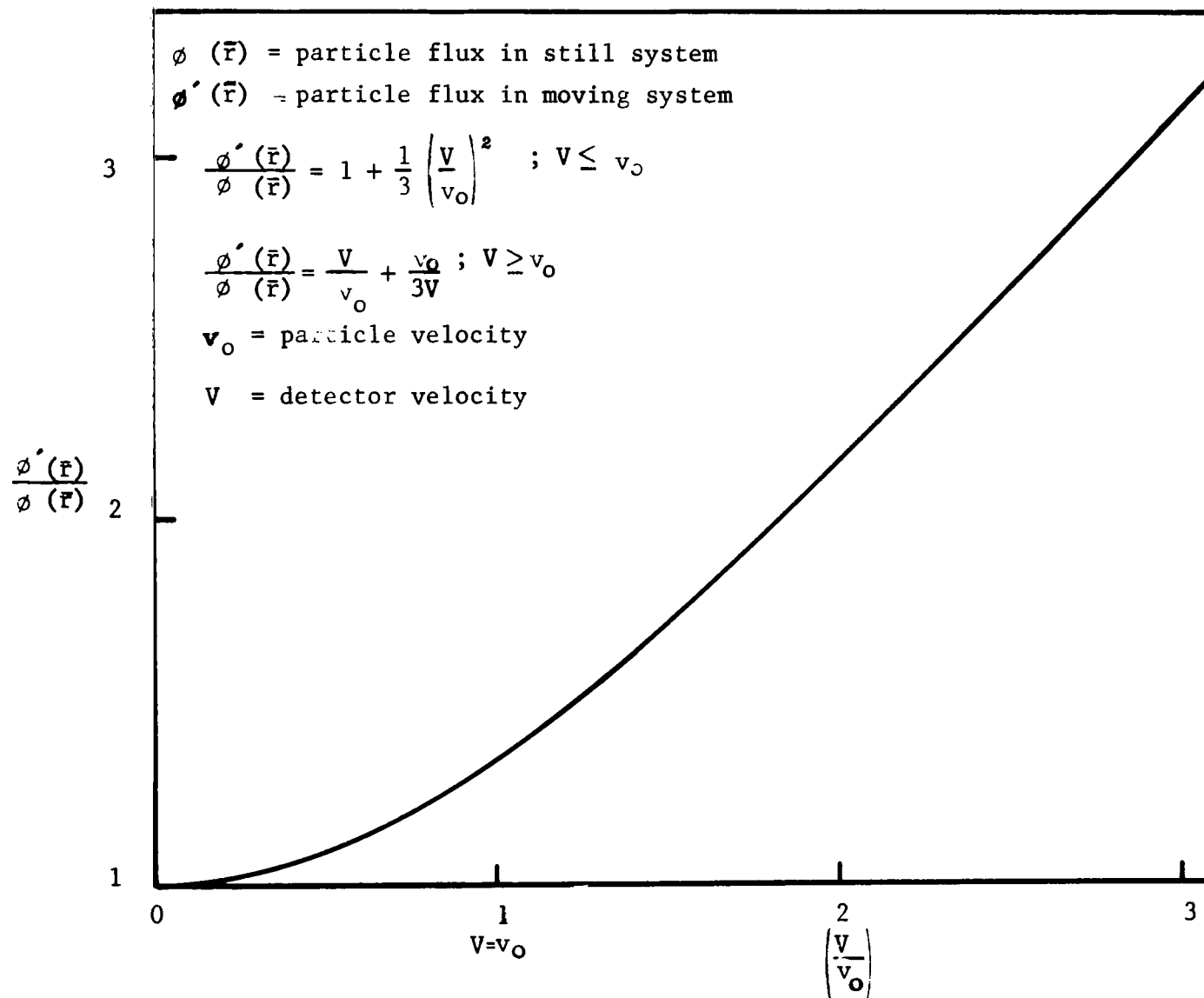


FIGURE 19. THE INFLUENCE OF DETECTOR MOTION ON APPARENT FLUX. THE DISTRIBUTION IN THE FIXED SYSTEM IS ASSUMED TO BE MONO-ENERGETIC, SPATIALLY UNIFORM, AND ISOTROPIC

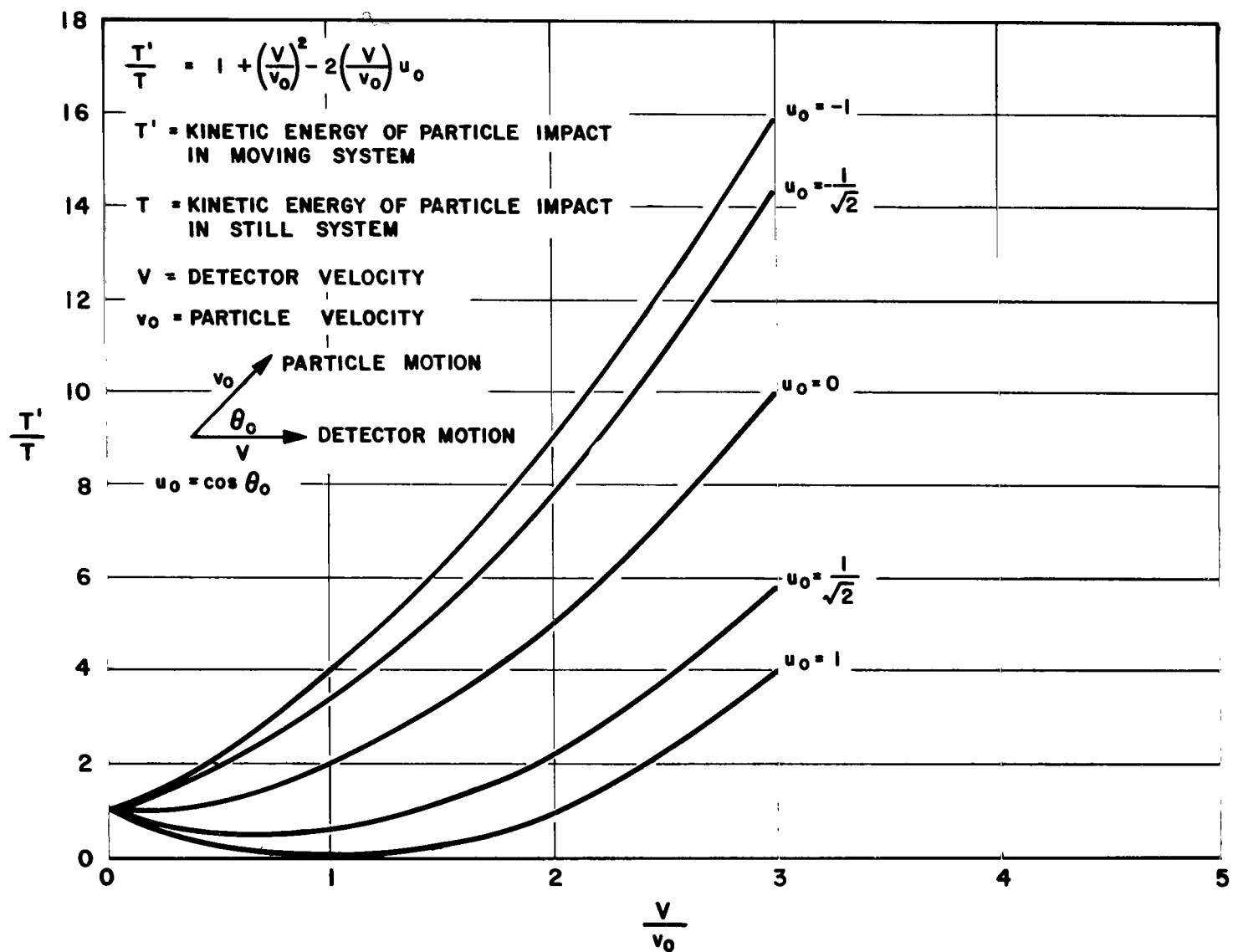


FIGURE 20. THE EFFECT OF DETECTOR MOTION ON THE KINETIC ENERGY FOR MONOENERGETIC, MONODIRECTIONAL FLUX

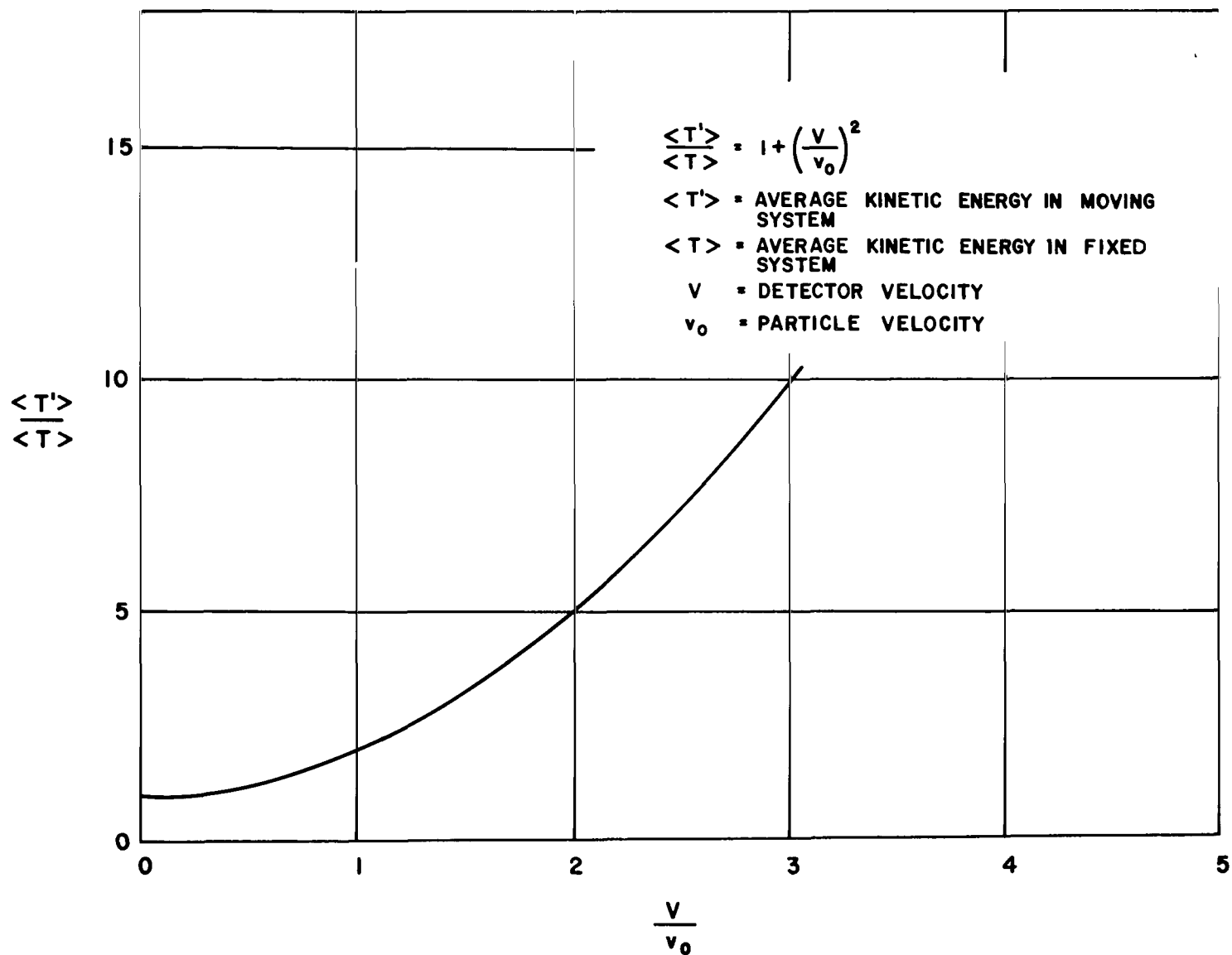


FIGURE 21. THE EFFECT OF DETECTOR MOTION ON THE AVERAGE KINETIC ENERGY FOR AN ISOTROPIC MONOENERGETIC DISTRIBUTION

A mathematical basis for discussing such subjects as the focusing of meteoroids by the earth has been provided, but considerable work still remains on the problem of using measured distributions, with no velocity or direction information, to estimate the meteoroid flux at infinity.

2/10/58
00

"The aeronautical and space activities of the United States shall be conducted so as to contribute . . . to the expansion of human knowledge of phenomena in the atmosphere and space. The Administration shall provide for the widest practicable and appropriate dissemination of information concerning its activities and the results thereof."

—NATIONAL AERONAUTICS AND SPACE ACT OF 1958

NASA SCIENTIFIC AND TECHNICAL PUBLICATIONS

TECHNICAL REPORTS: Scientific and technical information considered important, complete, and a lasting contribution to existing knowledge.

TECHNICAL NOTES: Information less broad in scope but nevertheless of importance as a contribution to existing knowledge.

TECHNICAL MEMORANDUMS: Information receiving limited distribution because of preliminary data, security classification, or other reasons.

CONTRACTOR REPORTS: Technical information generated in connection with a NASA contract or grant and released under NASA auspices.

TECHNICAL TRANSLATIONS: Information published in a foreign language considered to merit NASA distribution in English.

TECHNICAL REPRINTS: Information derived from NASA activities and initially published in the form of journal articles.

SPECIAL PUBLICATIONS: Information derived from or of value to NASA activities but not necessarily reporting the results of individual NASA-programmed scientific efforts. Publications include conference proceedings, monographs, data compilations, handbooks, sourcebooks, and special bibliographies.

Details on the availability of these publications may be obtained from:

SCIENTIFIC AND TECHNICAL INFORMATION DIVISION
NATIONAL AERONAUTICS AND SPACE ADMINISTRATION
Washington, D.C. 20546